

AD-A126 804

RIA-83-U242

IDE-TH-2005

AD A-126 804  
**TECHNICAL  
LIBRARY**

March 1983

## Low-Cost Stator Material for M734 Alternators

Jonathan E. Fine



**U.S. Army Electronics Research  
and Development Command  
Harry Diamond Laboratories**

Adelphi, MD 20783

The findings in this report are not to be construed as an official Department of the Army position unless so designated by other authorized documents.

Citation of manufacturers' or trade names does not constitute an official indorsement or approval of the use thereof.

Destroy this report when it is no longer needed. Do not return it to the originator.

UNCLASSIFIED

SECURITY CLASSIFICATION OF THIS PAGE (When Data Entered)

REPORT DOCUMENTATION PAGE		READ INSTRUCTIONS BEFORE COMPLETING FORM												
1. REPORT NUMBER HDL-TR-2005	2. GOVT ACCESSION NO.	3. RECIPIENT'S CATALOG NUMBER												
4. TITLE (and Subtitle)  Low-Cost Stator Material for M734 Alternators		5. TYPE OF REPORT & PERIOD COVERED Technical Report												
		6. PERFORMING ORG. REPORT NUMBER												
7. AUTHOR(s)  Jonathan E. Fine		8. CONTRACT OR GRANT NUMBER(s)												
9. PERFORMING ORGANIZATION NAME AND ADDRESS Harry Diamond Laboratories 2800 Powder Mill Road Adelphi, MD 20783		10. PROGRAM ELEMENT, PROJECT, TASK AREA & WORK UNIT NUMBERS  Program Element: P												
11. CONTROLLING OFFICE NAME AND ADDRESS U.S. Army Armament Research and Development Command Dover, NJ 07801		12. REPORT DATE March 1983												
		13. NUMBER OF PAGES 53												
14. MONITORING AGENCY NAME & ADDRESS (if different from Controlling Office)		15. SECURITY CLASS. (of this report)  UNCLASSIFIED												
		15a. DECLASSIFICATION/DOWNGRADING SCHEDULE												
16. DISTRIBUTION STATEMENT (of this Report)  Approved for public release; distribution unlimited.														
17. DISTRIBUTION STATEMENT (of the abstract entered in Block 20, if different from Report)														
18. SUPPLEMENTARY NOTES  HDL Project: 406846, 406946 DRCMS Code: 41111620J07														
19. KEY WORDS (Continue on reverse side if necessary and identify by block number)  <table border="0"> <tr> <td>Alternator</td> <td>Wind energy for fuze</td> <td>Environmental signature</td> </tr> <tr> <td>Air-driven generator</td> <td>Stator materials</td> <td>Permanent magnet alternator</td> </tr> <tr> <td>Battery</td> <td>Fuze power supply</td> <td>Lightweight company mortar system</td> </tr> <tr> <td>Power supply</td> <td>Multioption mortar fuze</td> <td>Safety and arming</td> </tr> </table>			Alternator	Wind energy for fuze	Environmental signature	Air-driven generator	Stator materials	Permanent magnet alternator	Battery	Fuze power supply	Lightweight company mortar system	Power supply	Multioption mortar fuze	Safety and arming
Alternator	Wind energy for fuze	Environmental signature												
Air-driven generator	Stator materials	Permanent magnet alternator												
Battery	Fuze power supply	Lightweight company mortar system												
Power supply	Multioption mortar fuze	Safety and arming												
20. ABSTRACT (Continue on reverse side if necessary and identify by block number)  <p>The M734 multioption mortar fuze employs an air-driven alternator to power the fuze electronics and to furnish a mechanical arming signature. The stator of the alternator is fabricated from an expensive high-nickel-content steel, Permalloy, costing \$6.00 per pound. The two-piece stator is stamped in production quantities from progressive dies. A product improvement program was initiated to find a lower cost substitute stator material from the silicon steel family costing only \$0.50 per pound.</p>														

## 20. ABSTRACT (Cont'd)

The program results showed that the nickel-coated M-36 silicon electrical steel is a suitable substitute for the Permalloy presently used in the alternator stator with respect to gun ruggedness, electrical output in flight, corrosion resistance, and voltage and frequency parameter adjustment. However, differences in stamping and drawing properties from those of Permalloy affect the end-plate and housing contact surface and the ability to draw the cup that contains the bearing. These differences required corrective assembly procedures. To eliminate this corrective assembly, production dies must be developed that allow for the stamping and drawing properties of the electrical steel. The cost of developing these dies could be amortized during a mobilization, but is not warranted with the production buys now anticipated. The cost and time to develop these dies are not compatible with the present production schedule. However, this material should be considered as a substitute material in the event of a mobilization base action.

## CONTENTS

	<u>Page</u>
1. INTRODUCTION .....	7
2. PERFORMANCE REQUIREMENTS OF ALTERNATOR AS FUZE POWER SUPPLY ....	9
2.1 Magnetic Circuit .....	9
2.2 Electrical and Magnetic Properties .....	10
2.2.1 Permalloy 49 .....	10
2.2.2 Electrical Steel .....	11
2.3 Mechanical Properties .....	13
2.4 Heat Treatment .....	13
2.5 Protective Coatings .....	14
2.6 Alternator Assembly and Calibration .....	14
3. PRELIMINARY RESULTS .....	16
3.1 First Results .....	16
3.2 Effect of Reducing Magnet Length .....	17
3.3 Effect of Heat Treating .....	18
3.4 Effect of Coating .....	18
3.5 Summary of Preliminary Results .....	18
4. STAMPING RUN OF 200 STATOR SETS .....	19
4.1 Producibility .....	19
4.2 Performance Characteristics of Alternators Manufactured with M-36 Silicon Steel .....	20
4.3 Annealing Study .....	21
5. EFFECT OF TEMPERATURE AND HUMIDITY CYCLING ENVIRONMENT ON EXPOSED ALTERNATORS HAVING M-36 ELECTRICAL STEEL STATORS .....	22
6. ASSEMBLY OF ELECTRICAL STEEL STATOR ALTERNATORS FOR FIELD TEST .....	26
6.1 Results of Assembly at Alternator Contractor .....	26
6.2 Examination of Parts at HDL .....	26
6.3 Corrective Measures .....	28
6.4 Effect of Tight Shaft on Parameter Adjustment .....	29
6.5 Condition of Alternators Assembled at HDL for Field Test .	29
7. FIELD TEST RESULTS ON NICKEL-COATED STATOR ALTERNATORS .....	30
8. CONCLUSIONS AND RECOMMENDATIONS .....	31
ACKNOWLEDGEMENTS .....	50
DISTRIBUTION .....	51

## APPENDICES

	<u>Page</u>
A.--ALTERNATOR PARAMETER ADJUSTMENT .....	33
B.--EXAMINATION OF TURBOALTERNATORS USED IN TEMPERATURE AND HUMIDITY TEST .....	45

## FIGURES

1. Low-cost stator alternator design .....	8
2. Magnetic circuit of alternator showing flux path .....	10
3. Magnetizing fixture .....	15
4. Apparatus for calibrating alternator in laboratory .....	16
5. T&H test units after 14 days .....	24
6. T&H test units after 28 days .....	24
7. Cross section of stator assembly showing critical interfacing surfaces, alignments, and magnetic flux path .....	27
8. Comparison of end plate and housing interface for Permalloy and M-36 .....	28

## TABLES

1. Electrical and Mechanical Properties of Permalloy and Electrical Steels .....	11
2. Comparison of Output of Alternators Having Several Stator Materials .....	17
3. Effect of Rotor Length on Output of Alternators of Several Casing Materials and Coatings .....	17
4. Effect of Stress-Relief Anneal on Alternator Output .....	18
5. Effect of Protective Coatings on Annealed Stators .....	18
6. Results of HR30T Hardness Measurements Made by NBS .....	19
7. Output of Sample of Uncoated Alternators from Batch of 200 Stamped with Progressive Dies .....	20
8. Output of Sample of Nickel-Coated Alternators from Batch of 200 Stamped with Progressive Dies .....	21

TABLES (Cont'd)

	<u>Page</u>
9. Data on Coated and Uncoated M-36 Stator Alternators Before Temperature and Humidity Cycling Test .....	23
10. Comparison of Alternator Output Before and After Temperature- Humidity Cycling Test .....	25
11. Summary of Field Test Data on Low-Cost Stator Material .....	31

## 1. INTRODUCTION

The M734 multioption mortar fuze developed for use on the new Army Lightweight Company Mortar System employs a ram-air-driven alternator as the power supply. The alternator provides air velocity as a second safety signature to satisfy MIL-STD-1316A, which requires dual safety signatures for all ammunition. Air during flight is directed to a turbine mounted on a shaft that is common to a concentrically mounted permanent magnet rotor. The spinning turbine drives the magnet to switch the flux through a Permalloy stator that surrounds a coil. This generates electricity to power the fuze electronics. In addition, the concentric shaft extends through the alternator and terminates in a screwdriver-like slot that engages with the safety and arming (S&A) system. This arrangement drives a gear train that unlocks the rotor. After mechanical arming occurs, usually within the first second of flight, the alternator shaft is released from the S&A to provide full electrical power. Thus, the alternator provides both mechanical and electrical energy for the fuze.

The alternator design has evolved from a laboratory model, made from screw-machine parts and expensive miniature precision bearings, to the present low-cost production design. In this version (fig. 1), the two-piece stator casing (labeled "housing" and "end plate") is stamped on a progressive die, the bearings are also stamped, and the shaft which forms the bearing inner race is cold formed. The cast-and-ground magnet is molded with a thermoplastic onto the shaft. The turbine and bobbin are molded from nylon, and the coil is a simple winding. This has resulted in a low-cost design that is the state of the art in fuze technology. To date, about 300,000 units have been produced.

A further cost savings could be achieved if a less costly stator material could be found. The present material, Permalloy, also known as Hi-Perm 49, contains iron mixed with 49-percent nickel. Because of the high cost of nickel, this material is expensive and at the beginning of this program sold for \$2.35 per pound, compared with \$0.35 per pound for the more common silicon electrical steels that are used in transformer laminations. Since eight complete stators are produced from each pound of material, the use of silicon electrical steel would produce a \$0.25 savings in material cost alone for each alternator. This savings was the motivation behind this product improvement program (PIP). Now the cost of Permalloy has increased to about \$6.00 per pound, while the electrical steels are sold for \$0.45 per pound. Thus the incentive to find a low-cost stator material is now even stronger.

The approach used was to conduct in the laboratory a preliminary screening on several silicon steel materials and coatings. The materials were selected on the basis of their electrical and magnetic properties. Sample units of each material were stamped on production-like dies, assembled into alternators, and evaluated in laboratory performance tests. Units made from selected silicon steels were coated with various protective materials such as nickel, cadmium, and zinc before assembly.



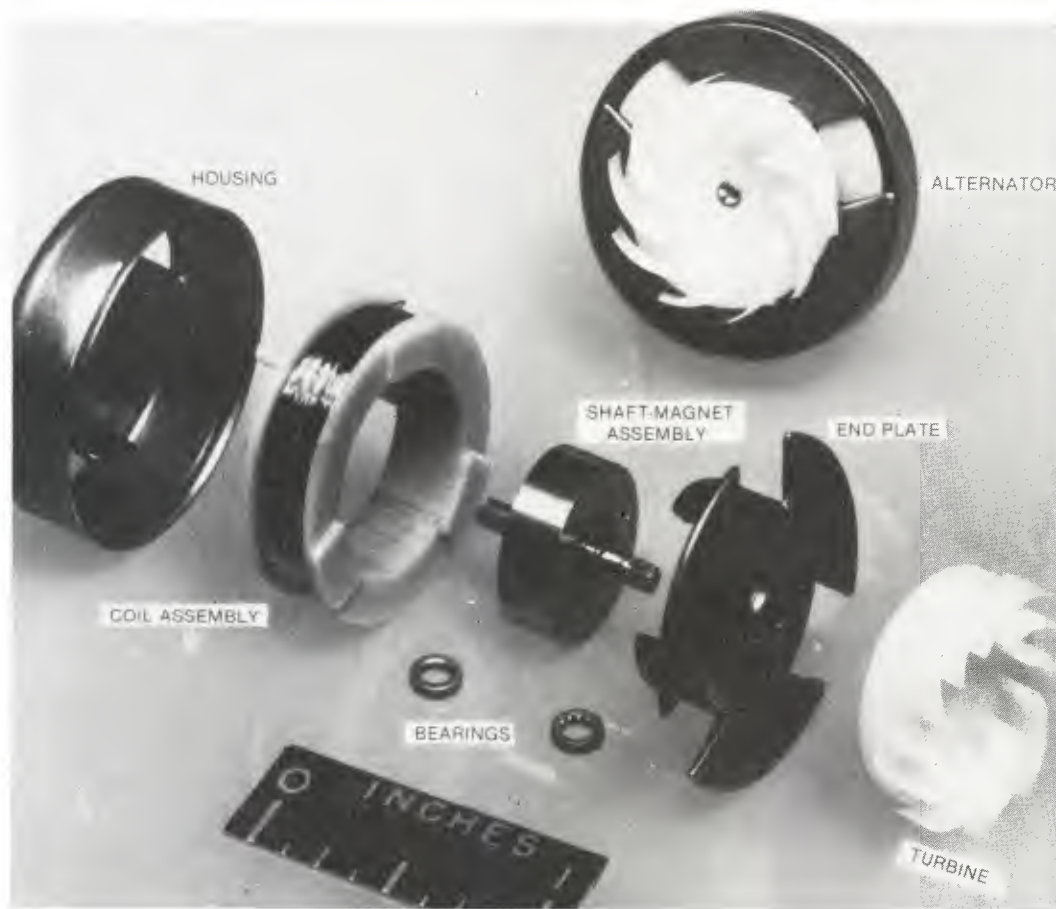


Figure 1. Low-cost stator alternator design.

From the above procedure, a larger sample of the more promising materials was stamped, fabricated, and coated with nickel, cadmium, or zinc in the laboratory.

Upon completion of the laboratory investigation, our plan was to have all stamping and assembly of units done by the contractor in his plant (Alinabal Corp., Milford, CT) according to existing manufacturing procedures. These units would then be assembled into fuzes by the fuze contractor (Eastman Kodak, Rochester, NY) and field tested. The intent is to achieve a reliable comparison with the presently used Permalloy material.

Several factors impeded this plan. The first was that the automated progressive dies could not be used to stamp the silicon steel because they were undergoing prove-out. As a result, the preliminary tests in the screening process were done on units stamped from manually operated dies and presses. Midway through the program, the stator dimensions were modified slightly in the prove-out process of the progressive dies, so that shaft magnet assemblies already on hand for the PIP did not fit the new parts. Since the stamping properties of the electrical steels are different from those of Permalloy, this resulted in some distortion in the parts stamped from the electrical steel. These distortions caused mechanical interferences that masked material differences, and had to be recognized and corrected before a proper assessment of the electrical steels could be made. Finally, a delay in the entire fuze program prevented receiving fuzes and projectiles on schedule for an earlier planned field test. Production, which was already behind schedule, took precedence over the PIP.

Nevertheless, the results discussed below do show that a low-cost material could be used as a substitute for the Permalloy after stamping dies are developed. The dies that stamp Permalloy and silicon steels cannot be used interchangeably.

## 2. PERFORMANCE REQUIREMENTS OF ALTERNATOR AS FUZE POWER SUPPLY

The PIP had the objective of finding a suitable substitute low-cost stator material among the silicon steel family that would

- (1) match or improve the electrical output of the production alternator without affecting the mechanical output,
- (2) allow demagnetization adjustment to achieve the proper frequency range and still produce the required voltage,
- (3) retain the mechanical strength to maintain the alignment and engagement with the S&A,
- (4) be producible from the existing progressive dies, and
- (5) require no modification of other alternator or fuze components.

To accomplish these objectives, it was necessary to consider material properties, assembly, and calibration (parameter adjustment) procedures.

### 2.1 Magnetic Circuit

The relationship between the electromagnetic and mechanical properties of the alternator is determined by the magnetic circuit of the alternator. Air during flight impinges on the turbine of the alternator and produces rotational motion of the shaft. The magnetic circuit containing the magnet rotor, a six-pole stator, and a coil converts the rotational motion to electrical energy.

The rotor consists of a magnet with six poles and is centrally located between the pole pieces of the stator (fig. 2). Each casing (housing and endplate shown in fig. 1) contains three pole pieces separated by  $120^\circ$  between centers. The stator end plate is assembled into the housing, so that the separation between the centers of any two adjacent pole pieces is  $60^\circ$ . In this assembly, the coil subassembly fits between the end plate and housing.

As the turbine wheel rotates, the magnetomotive force of the magnet transfers flux through the stator, and an electromotive force (emf) is induced in the coil winding. For every  $120^\circ$  of rotation, the induced emf completes one electrical cycle.

As seen in figure 2, the flux paths have different directions through the stator; hence, only nonoriented materials have been considered for this application.

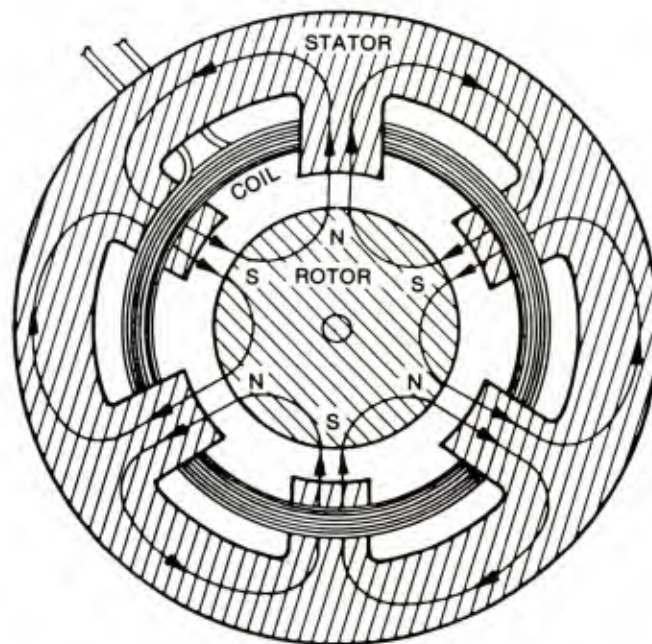


Figure 2. Magnetic circuit of alternator showing flux path.

## 2.2 Electrical and Magnetic Properties

### 2.2.1 Permalloy 49

For the present M734 alternator, the stator casing material, which must conduct the rotor magnetic flux through the coil, is Permalloy 49, an iron alloy containing 49-percent nickel. This material has a high saturation flux density, but a much lower hysteresis loss coefficient than soft iron. The electrical resistivity of Permalloy 49 is higher than soft iron so that eddy-current losses are reduced. Thus, a high saturation flux density, com-

parable to iron, and low core losses are the most important electrical properties of any candidate material. Because the magnetic flux reverses direction periodically through the stators, the initial permeability is also an important property.

The material properties of the stator affect both the electrical output of the alternator and the ability to adjust within the desired frequency range. These material properties, which are obtained from the manufacturer, are determined from tests performed at standard operating conditions on samples having standard shapes: either a flat ring or a flat strip. These standards are uniform throughout the industry. The extension of the data to a real design that has a different shape and different operating conditions is not usually obvious.

Other properties such as saturation flux density, resistivity, and core loss are typical properties that can be used to compare various materials, since they correspond to the same shapes and operating conditions. Table 1 displays values from the literature for Permalloy and several candidate materials.

TABLE 1. ELECTRICAL AND MECHANICAL PROPERTIES OF PERMALLOY AND ELECTRICAL STEELS

Material	Nominal silicon content	Saturation flux density	Core losses [(W/lb)/cycle]	Resistivity ( $\mu\Omega$ -cm)	Coercive force at 10 kG (Oe)		
Permalloy	-	15.5	0.0125	50	0.03		
M-22	3%	19.7	*0.035	46	0.54		
M-36	1.4%	20.2	*0.04	44	0.34		
M-43	0.95%	20.3	*0.051	28	0.80		
M-45	1.5%	20.7	*0.06	32	-		
	Permeability at 15 kG	Curie temperature (F)	Density (lb/in. <sup>2</sup> )	Hardness (Rockwell B)	Ultimate tensile strength (psi)	Tensile yield strength (psi)	
Permalloy	1,500	840	0.298	40	64,000	22,000	
M-22	1,276	1350	0.276	80	71,000	54,000	
M-36	1,724	-	0.28	74	68,000	47,000	
M-43	1,875	1360	0.28	66	65,000	46,000	
M-45	2,055	-	0.28	55	55,000	35,000	

\*At 60 Hz, 15 kG.

### 2.2.2 Electrical Steel

The electrical steels are mostly iron with 1.5- to 3-percent silicon and traces of other metals. Silicon increases the material hardness and the electrical resistivity.



The electrical steels M-22 through M-45 are used in transformer laminations for motors and generators of various sizes, ranging from fractional-horsepower motors and small appliance motors to large electric power generators. The material for many of these applications is arranged in laminations with a thin layer of electrical insulation between the laminations. They are rated according to core losses, which include hysteresis loss, eddy-current loss, and interlamination loss. For example, the M-22 has a lower core loss than the M-45.

The silicon content, and consequently the material hardness, may vary from one batch to another within a given rating (see table 1).

Saturation flux density indicates the maximum density of flux that the magnet can push through the useful flux path in the stator material. Additional flux goes into leakage and therefore does not cut the coil to produce voltage. Measurements of open-circuit voltage for alternators indicate that the flux level within the minimum cross section of any stator pole is 5,000 to 10,000 G,\* which is below the saturation flux density of 15,500 G for Permalloy. All the electrical steels have higher saturation flux densities--about 20,000 G, which is greater than that of Permalloy. Hence, the new materials do not reduce the flux-carrying capacity of the stator, but in fact limit it even less.

The resistivity is the resistance to eddy-current losses within the stator. More resistive materials have lower eddy-current losses. Permalloy has a resistivity of 50  $\mu\Omega$ -cm; M-22 and M-36 are close with values of 46 and 44  $\mu\Omega$ -cm, respectively, and therefore should have the same eddy-current losses as Permalloy. M-43 and M-45 have much lower resistivities, and should therefore be much higher in eddy-current losses.

The core loss coefficient lumps together the combined effect of hysteresis and eddy-current losses. The loss coefficient for Permalloy is about half the value for the electrical steels. Thus the core losses for the electrical steels would be about twice again higher than those for Permalloy at the same operating frequency and flux density. This is a major difference in the electrical properties of the materials.

A second major difference is in the coercive force required to produce 10 kG. Permalloy requires a much lower coercive force (0.03 Oe†) to produce a flux density of 10 kG than the electrical steels. M-36, the best coercive material of the electrical steels, is 10 times worse (0.3 Oe) in this respect.

---

\* (gauss)  $10^{-4}$  = (tesla)

† (oersteds) 79.58 = (amperes per meter)

### 2.3 Mechanical Properties

The mechanical properties of the electrical steels compared with Permalloy are also shown in table 1. The density, hardness, and yield strength indicate that the electrical steel properties are directly dependent on silicon content.

The density of the electrical steels is 8 percent less than Permalloy. Permalloy, having a hardness of RB 40 (40 on the Rockwell B-scale) is softer than the electrical steels. The hardness increases with silicon content from RB 55 for M-43 to RB 80 for M-22.

The ultimate tensile strength also increases with silicon content from 55 kpsi\* for M-45 to 64 kpsi for M-22. The strength of Permalloy is 64 kpsi, which is comparable to M-43.

The tensile yield strength is less for Permalloy than for the electrical steels.

These differences in hardness and strength are related to the differences in stamping properties between Permalloy and the electrical steels and among the various types of electrical steel.

In summary, the properties of the silicon steels are in the same range as those of Permalloy.

### 2.4 Heat Treatment

All the stator materials, including Permalloy, must be properly heat treated to develop the optimum electrical properties. The heat treatment also affects the material hardness and its stamping properties.

Permalloy requires a long heat-treating process after stamping and drawing. This optimizes electrical and magnetic properties and relieves stresses in manufacture. The process must maintain a gradual cooling rate that establishes the proper grain structure. The maximum temperature is 2150 F† for four hours, and the maximum cooling rate is 150 F per hour down to 1100 to 1150 F, and not above 220 F per hour down to 650 F. The hardness after annealing is RB 40. This process takes about 12 to 14 hours. A dry hydrogen atmosphere is preferred to remove carbon from the surface of the material. However, a vacuum anneal has proved satisfactory.

The silicon electrical steels are fully processed by the manufacturer, but require a short stress-relief anneal after stamping and drawing are completed. For this process the maximum temperature is 1550 to 1650 F for one hour, and the cooling rate is not critical. Cracked gas or dry nitrogen is the preferred atmosphere to promote decarbonizing of the surface. This is instrumental in achieving the optimum electrical and magnetic properties.

---

\* (psi)  $6.895 \times 10^3 =$  (pascals)

†  $[(F) - 32] \ 5/9 = (C)$

## 2.5 Protective Coatings

The high rust and corrosion resistance of Permalloy results from its high nickel content. Silicon electrical steel, on the other hand, must be protectively coated. The most promising coating materials are cadmium, zinc, and nickel. These materials are commonly used in industry to protect steel and can be electrodeposited in a batch process. Slight variations in composition do not reduce the protection against corrosion in the atmosphere.

Cadmium protects against alkalis and sea water. It has a very slow corrosion rate in outdoor atmosphere, and in oxygen-containing atmosphere it protects sacrificially. That is, the coating itself oxidizes and forms a protective shield over the material being protected. Cadmium is susceptible to sulfur dioxide in the atmosphere, and it will corrode when exposed to certain unsaturated oils in enclosures without air circulation. It can form a galvanic reaction with other metals with which it may come in contact.

Zinc's primary industrial use is in controlling the corrosion of steel. It protects sacrificially, as does cadmium, and resists atmospheric corrosion and corrosion within moving water. The corrosion in stagnant water is accelerated by the presence of dissolved gases. Zinc corrodes rapidly with acids and strong alkali solutions. Galvanic properties where zinc contacts other metals are similar to cadmium.

Nickel provides resistance to a wide range of atmospheres and substances. These include various indoor and outdoor atmospheres, salt water, cleaning solutions, foods, and beverages. The total corrosion of the base metal may be reduced as much as possible by increasing the thickness of the plating material. The thickness and not the method of plating is important. Nickel does not protect sacrificially; hence, the initial coating must be complete and unbroken.

Typical plating thickness for any of these materials is 0.2 to 1.5 mil.\*

An electroless nickel plating method has the advantage of plating uniformly in the bearing boss and at the interface where the end plate and housing come together (fig. 1).

Thus, nickel has the most advantages as a protective coating and was used with the selected stator material.

## 2.6 Alternator Assembly and Calibration (Parameter Adjustment)

The assembly operations which can affect the electrical operation of the alternator are listed below:

- (a) magnetizing the rotor,

---

\* (mil) 0.0254 = (mm)

- (b) inserting the rotor into the housing,
- (c) installing the end plate, and
- (d) demagnetizing the alternator in a controlled manner.

All subassembly operations, such as installing bearings in stators and coil assembly in housings, are completed before the above operations. The turbine is added between steps (c) and (d).

The rotor, initially unmagnetized, is inserted into a fixture as shown in figure 3. A magnetizing pulse is applied to all six coils and it induces the 6-pole configuration shown in figure 2. The magnetizing current is sufficient to saturate the magnet. The magnet is removed from the magnetizing fixture and is installed in the stator assembly. The turbine is then placed on the alternator shaft; now the fully assembled alternator is ready to be adjusted.

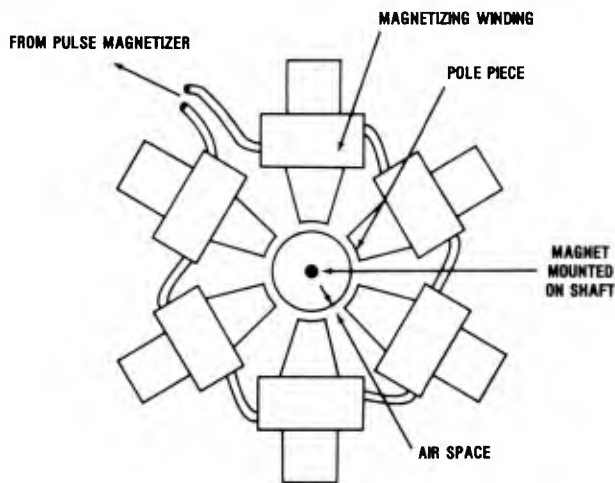


Figure 3. Magnetizing fixture.

The purpose of the adjustment is to achieve a rotational speed at a set inlet pressure that will provide the required safe arming distance. Higher frequencies than specified will arm the fuze when fired at high charge zones before safe separation from the gun has occurred. Lower frequencies will cause late arming at the low charge zones. Thus, the mechanical operation of the fuze is related to the electrical properties of the alternator. Hence, a must requirement of any new stator material is that it allow the alternator to be adjusted to within the appropriate rotational speed range and still produce the required voltage level.

The alternator is inserted in the calibrating fixture shown schematically in figure 4. Air at constant pressure is applied to the ogive containing the alternator. A resistive load of 600  $\Omega$  is used. Voltage and frequency are monitored.



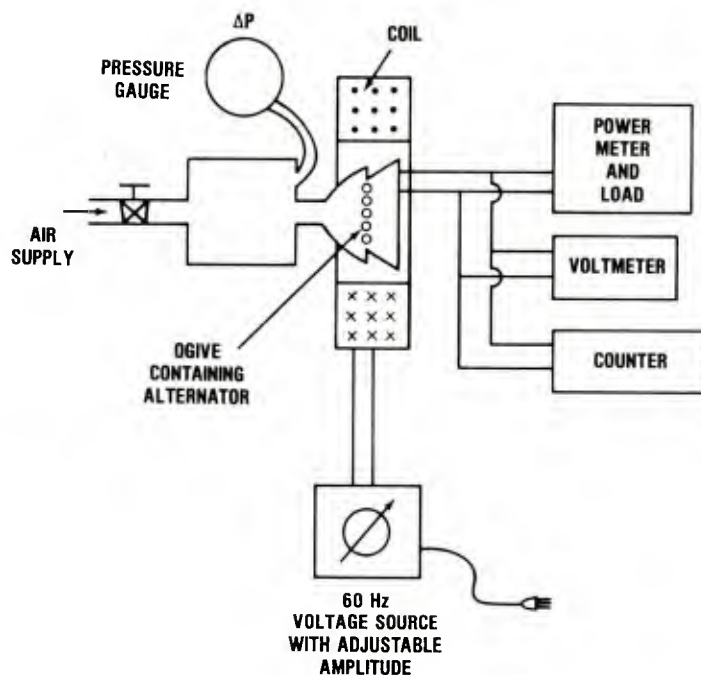


Figure 4. Apparatus for calibrating alternator in laboratory.

The application of a programmed voltage to the adjustment coil sets up a magnetic field that slightly demagnetizes the spinning rotor. This lowers the flux density through the coil and the magnetic attraction between the stator and the magnet, so the rotational speed increases. The voltage also increases because the increase in the time rate of change of flux offsets the decrease in flux. Eventually a point is reached, with further increases in demagnetization signal, at which the increase in rotational speed no longer compensates for the decrease in flux, so that the voltage is reduced. Thus both the frequency and voltage of an alternator are adjusted to the required range.

Further discussion of parameter adjustment is included in appendix A.

### 3. PRELIMINARY RESULTS

#### 3.1 First Results

At the start of the program, samples of several stator materials were obtained from the contractor. These samples, containing coated and noncoated stators, were assembled into alternators and their performance was found to be inadequate (table 2).

TABLE 2. COMPARISON OF OUTPUT OF ALTERNATORS  
HAVING SEVERAL STATOR MATERIALS

Stator material	Coating	Alternator number	Conditions at 0.206 psig	
			Freq (Hz)	Volts (rms)
Permalloy	None	M-69	1410	22.5
		M-71	1395	22.4
		M-75	1390	22.6
		M-76	1415	22.6
		M-77	1415	21.9
		M-78	1360	22.5
M-36	None	T-1	1505	20.4
	Cadmium	T-4	1479	18.7
	Cadmium	T-5	1358	20.0
	Nickel	T-2	1356	18.3
	Nickel	T-3	1370	17.0
M-43	None	T-6	1356	19.2
	None	T-7	1359	20.0
	Cadmium	T-8	1381	18.5
	Cadmium	T-9	1461	18.0
	Nickel	T-10	1455	19.4
	Nickel	T-11	1343	19.6
	Zinc	T-12	1376	18.7
	Zinc	T-13	1384	18.3

The voltages measured at a pressure of 0.206 psig\* range from 18.0 for M-43 coated with cadmium to 19.4 V for M-43 coated with nickel and 20.4 V for uncoated M-36. All these values were below the required 21.0 V into a 600- $\Omega$  load. From these data all materials and coatings appear to perform about the same.

### 3.2 Effect of Reducing Magnet Length

The lower performance was attributed to large core losses which are greater at the higher flux densities. Hence several magnet rotors were ground down to different lengths to see if lower flux levels would also reduce the core losses. The results are shown in table 3.

For M-36, reducing the magnet length from 0.200 to 0.183 in. achieved 21.0 V at 1357 Hz. A further reduction to 0.165 in. resulted in an increase to 21.2 V at 1398 Hz. Voltage increase with reduction in magnet length was not dramatic.

TABLE 3. EFFECT OF ROTOR LENGTH ON OUTPUT OF ALTERNATORS OF SEVERAL CASING MATERIALS AND COATINGS

Alternator number	Casing material	Rotor length (in.)							
		0.165		0.175		0.183		0.200	
		Freq (Hz)	Volts (rms)	Freq (Hz)	Volts (rms)	Freq (Hz)	Volts (rms)	Freq (Hz)	Volts (rms)
T-16	Permalloy	1381	21.3	1419	21.5	1334	21.5	1407	21.8
T-1	M-36 uncoated	1398	21.2	1431	20.9	1357	21.0	1505	20.4
T-4	M-36 cadmium	1359	19.8	1366	19.6	-	-	1479	18.7
T-5	M-36 cadmium	1393	20.5	1368	20.7	-	-	1358	20.0
T-11	M-43 nickel	1372	19.9	1383	19.7	1351	20.2	1409	19.5

\*psig--differential pressure above ambient atmospheric pressure of 14.7 psi.

### 3.3 Effect of Heat Treating

The materials were heat treated according to manufacturers' specifications, and the data for the assembled alternators are compared with data for unannealed units in table 4. It can be seen that following heat treatment the two uncoated materials, M-36 and M-43, produce voltage and frequency values comparable to those of Permalloy.

### 3.4 Effect of Coating

The effect of nickel and cadmium coating on electrical output was then investigated. The results are shown in table 5. A voltage reduction of 0.7 to 0.8 V occurs for M-36 when coated with the nickel or cadmium, but the required output level is achieved.

TABLE 4. EFFECT OF STRESS-RELIEF ANNEAL ON ALTERNATOR OUTPUT

Description	Conditions at 0.206 psig			
	Before anneal		After anneal	
	Freq (Hz)	Volts (rms)	Freq (Hz)	Volts (rms)
M-36 uncoated	1333	19.0	1368	22.4
M-43 uncoated	1320	18.4	1324	22.4

TABLE 5. EFFECT OF PROTECTIVE COATINGS ON ANNEALED STATORS

Material	Frequency and voltage at 0.206 psig					
	Uncoated		Nickel coating		Cadmium coating	
	Freq (Hz)	Volts (rms)	Freq (Hz)	Volts (rms)	Freq (Hz)	Volts (rms)
Permalloy	1350	22.1	-	-	-	-
M-36	1300	22.2	1390	21.4	1309	21.5
M-43	-	-	-	-	1319	21.8

### 3.5 Summary of Preliminary Results

The above results were obtained on a small sample of five alternators made from each type of stator material. Usually fewer samples of a given coating were tested. However, these limited tests did indicate that these materials with protective coatings could meet the required performance level.

On the basis of these preliminary results, two of the more promising materials, M-36 and M-45, were selected to make a batch of 200 sets of stator parts for more extensive evaluation. Although M-43 had demonstrated adequate output, M-45 was a promising candidate according to published properties, but had not yet been evaluated. Locore-N had showed high output but was not investigated further because the required lamination thickness of 0.031 in. could not be obtained.

#### 4. STAMPING RUN OF 200 STATOR SETS

##### 4.1 Producibility

The 200 sets of M-36 stator parts and the 200 sets of M-45 stator parts were stamped by the alternator contractor using the progressive dies. The contractor reported that M-45 material was very difficult to stamp, especially the housings. A large number of rejects occurred before the set of 200 stators was completed, and considerable damage was caused to the dies.

Annealing was done on 25 sets of parts of each type, and a sample was sent to the National Bureau of Standards for micro-hardness measurements. The samples for each of the two materials included the material before stamping, an end plate and housing in the as-stamped condition, and an end plate and housing after annealing. The results in terms of Rockwell B equivalents are shown in table 6 and may be compared with the hardness values from table 1.

The M-36 material sample hardness was close to the value cited in the literature. The stamping operation did not affect the end plate noticeably, but the housing which is drawn into a cup appeared to be work-hardened to RB 83. Annealing softened both the end plate and housing to between RB 64 and 65.

The M-45 material sample was harder than the value given in the literature. The end plate did not change in stamping, whereas the housing, as with the M-36 material, was work-hardened. Annealing softened both the end plate and housing to the same hardness as the M-36 after annealing. The effect of stamping was more noticeable in the housing. The M-45 was work-hardened more than the M-36, which may account for the contractor's difficulty in stamping the material.

Because of the manufacturing difficulty with M-45, this material was eliminated from further consideration and M-36 was selected as the more promising material to evaluate extensively.

TABLE 6. RESULTS OF HR30T HARDNESS  
MEASUREMENTS MADE BY NBS

Test piece	Approximate Rockwell B equivalent hardness
M-36 Material sample	77
M-36 End plate, as stamped	75
M-36 Housing, as stamped	83
M-36 End plate, annealed	65
M-36 Housing, annealed	64
M-45 Material sample	64
M-45 End plate, as stamped	65
M-45 Housing, as stamped	81
M-45 End plate, annealed	64
M-45 Housing, annealed	64

#### 4.2 Performance Characteristics of Alternators Manufactured with M-36 Silicon Steel

Fourteen annealed and uncoated stator sets of M-36 were assembled into alternators and adjusted to the frequency range of 1300 to 1450 Hz. The voltage and frequency values are shown in table 7. All but three met the required voltage.

Four M-45 uncoated units also were assembled and adjusted, and are included in table 7. The average voltage for this group was lower than that of the M-36 units, and only two met the requirements.

Four additional M-36 alternators were coated with nickel by the electroless plating process.\* The frequency and voltage after parameter adjustment are given in table 8. The voltages still met the 21.0-V requirement, but were marginal. The average voltage for the coated group was 21.1 V compared with 21.3 for the uncoated group which is not statistically significant for the sample sizes used.

TABLE 7. OUTPUT OF SAMPLE OF UNCOATED ALTERNATORS FROM  
BATCH OF 200 STAMPED WITH PROGRESSIVE DIES

Description	Alternator number	After calibration at 0.206 psig	
		Freq (Hz)	Volts (rms)
M-36, stress-relief annealed, uncoated	36-1	1331	22.2
	36-2A	1328	21.3
	36-3	1384	21.2
	36-4A	1331	21.7
	36-5A	1310	20.8
	36-6	1389	20.6
	36-7	1333	20.5
	36-8	1340	21.7
	36-9	1343	21.1
	36-10	1368	21.5
	36-11	1395	21.5
	36-12	1345	21.0
	36-13	1328	21.5
	36-14	1322	21.5
Avg		1346 $\pm$ 26.8	21.29 $\pm$ 0.46
M-45, stress-relief annealed, uncoated	45-1	1364	21.5
	45-2	1367	20.6
	45-3	1347	21.1
	45-4	1347	20.9
Avg		1356 $\pm$ 10.7	21.02 $\pm$ 0.37

\*Don Wells of HDL carried out the electroplating.

During the assembly of alternators from the 200 sets of parts, it became clear that mechanical problems were preventing the realization of the high output voltages observed earlier in the project. The problem was caused by the buildup of coating in the bearing boss, preventing proper bearing fit. The bearing became overstressed when pressed in. This resulted in excessive bearing friction, which prevented the realization of the required voltage at the adjustment frequency. In production, the dies must be modified to allow for the buildup of coating. For these units, the coating was removed by a polishing technique from the bearing boss. This allowed for a proper mechanical bearing fit between the two stator pieces.

After this operation, two groups of annealed stator sets were selected from the lot of 200. One group, comprising 50 sets, was sent to the contractor for assembly into alternators. These units were intended for use in laboratory evaluation and field testing. A second group, 35 sets, was used for a temperature-humidity test to evaluate the effectiveness of the nickel coating. The temperature-humidity test is discussed in section 5.

TABLE 8. OUTPUT OF SAMPLE OF NICKEL-COATED ALTERNATORS  
FROM BATCH OF 200 STAMPED WITH PROGRESSIVE DIES

Description	Alternator number	After calibration at 0.206 psig	
		Freq (Hz)	Volts (rms)
M-36 Nickel coated	36-17	1344	21.0
	36-18	1331	21.2
	* 36-19	1366	21.1
	* 36-20	1322	21.2
	Avg	1340 $\pm$ 19.1	21.12 $\pm$ 0.095

\*Bearing hole enlarged after plating.

#### 4.3 Annealing Study

A test was conducted to optimize the annealing process around the manufacturers' recommended time and temperature of 1 hour at 1600 F.\* A group of M-36 stator sets from the lot of 200 was divided into five batches: one was not annealed, and the other four were annealed under different conditions of time and temperature. All processes were done in a decarbonizing nitrogen atmosphere. The processes were evaluated by assembling several uncoated alternators of each type, calibrating them within the proper frequency range, and comparing the output voltages. It was found that the optimum process was to anneal the parts for 1 hour at 1500 F. No improvement in voltage output was gained by going to a cycle of 2 hours, or to higher temperatures.

---

\*Fremont Ice of HDL carried out the heat-treating process.



## 5. EFFECT OF TEMPERATURE AND HUMIDITY CYCLING ENVIRONMENT ON EXPOSED ALTERNATORS HAVING M-36 ELECTRICAL STEEL STATORS

A test was conducted to determine the effect of a temperature and humidity (T&H) environment on alternator electrical output. These alternators had nickel-coated electrical steel statos. The 28-day T&H test was intended to induce corrosion and rust that is worse than that expected over the fuze lifetime. MIL-STD-331, Test 105.1, was chosen, in which a 24-hour cycling of temperature from -80 to +165 F and relative humidity from ambient to 95 percent is repeated on 28 successive days. Normally, power supplies are assembled in fuzes which are shipped mounted on a projectile and in protective containers, and hence exposed very little to the environment. However, for the laboratory test chosen, the alternators were placed in open plastic trays that were completely exposed to the environment in order to obtain excessive corrosion.

The alternators for the T&H test were fabricated from M-36 electrical steel statos which had been coated with about 0.0010-in. electroless nickel on the surface. The buildup of nickel within the bearing cup prevented proper installation of the bearing (previously discussed). To remedy this, the coating was polished off inside the bearing cup. The coating was not removed from the contact surfaces between the housing and the end plate. This insured that the magnetic properties of the alternator would be the same as those that may be manufactured during high-volume production. The alternators were assembled from bearings that had been lubricated in 15-percent (by volume) Anderol 401D and 85-percent Freon mixture before installation in the stator.

The alternators exposed to the 28-day T&H recycling procedure included 19 with M-36 nickel-coated statos, 9 with M-36 uncoated statos, and 9 with Permalloy (Hi-Perm 49) statos (used as controls). The Permalloy stator alternators were as supplied by the contractor, assembled and adjusted. One additional alternator of each type was removed after 14 days for examination of the corrosion in the first part of the test.

To furnish a basis for determining the effect of the conditioning environment on electrical output, the M-36 nickel-coated alternators were tested at two points before the T&H conditioning began: (a) the voltage and frequency into a 600- $\Omega$  load were measured at 0.206 psig, and (b) the voltage into the 600- $\Omega$  load was measured at 1300 Hz. For the M-36 uncoated alternators, only the data at 0.206 psig were taken. The Permalloy alternators were known before the test to have voltages of at least 21.0 V and frequencies above 1300 Hz at 0.206 psig.

Table 9 compares data before the T&H test for both nickel-coated-stator alternators and uncoated units. The frequencies and voltages of the uncoated alternators are within the required range. The coated alternators have low voltage values even though the coating was removed from the bearing boss before assembly. Most of the frequencies of the coated units are within the required range. These units were adequate for evaluating changes in the output that might result from the T&H test.

TABLE 9. DATA ON COATED AND UNCOATED M-36 STATOR ALTERNATORS  
BEFORE TEMPERATURE AND HUMIDITY CYCLING TEST

Nickel coated					Uncoated		
Alternator number	Test with pressure at 0.206 psig		Test with frequency at 1300 Hz		Alternator number	Test with pressure at 0.206 psig	
	Frequency (Hz)	Volts (rms)	$\Delta P^*$ (psig)	Volts (rms)		Frequency (Hz)	Volts (rms)
36-17	1411	21.0	0.20	20.4	36-50	1321	21.6
36-18	1351	21.0	0.201	20.7	36-51	1332	21.1
36-20	1259	20.8	0.21	21.1	36-52	1356	21.4
36-21	1402	20.4	0.195	19.8	36-53	1342	21.6
36-22	1266	20.7	0.211	20.9	36-54	1332	21.3
36-32	1316	21.1	0.205	21.1	36-55	1330	21.5
36-33	1344	20.0	0.20	18.9	36-56	1332	21.2
36-34	1278	21.0	0.21	21.2	36-57	1319	21.8
36-35	1329	20.7	0.205	20.5	36-58	1346	21.4
36-36	1320	21.0	0.206	20.9	36-62	1341	21.2
36-37	1243	20.9	0.212	21.3			
36-38	1309	21.0	0.205	21.0			
36-39	1304	20.7	0.204	20.7			
36-40	1310	20.7	0.205	20.7			
36-41	1309	20.9	0.205	20.8			
36-42	1301	20.9	0.21	20.9			
36-43	1296	21.3	0.209	21.3			
36-44	1300	21.2	0.208	21.2			
36-46	1301	21.0	0.209	21.0			
36-47	1414	20.6	0.196	20.0			
36-48	1379	20.3	0.196	19.8			
36-49	1353	20.2	0.201	19.9			
Avg 1322 $\pm$ 47		20.79 $\pm$ 0.32			1335 $\pm$ 11		21.41 $\pm$ 0.22

\*Differential pressure

Figure 5 shows three alternators, one of each type, after 14 days of recycling. Considerable scale appears on the uncoated M-36 alternator (left), and a few small rust spots on the nickel-coated unit (right). The Permalloy control (center) had no noticeable marks. During part of each cycle, the alternators in the trays are removed from the chamber and placed on a table at ambient conditions for one hour. This affords time for a visual inspection of the units without disturbing the test. During the first two weeks of the test, the alternators were observed daily. Most of the visible corrosion occurred within the first few days of the tests, and did not change much on successive days. The appearance after 14 days is quite similar to that after completion of the test, as shown in figure 6.

An electrical continuity test was performed on the alternators after the T&H conditioning. This involved using an ohmmeter to measure the resistance between two points on the alternator, one on the housing and the other on the end plate. Before the T&H conditioning, an ohmmeter typically would read zero resistance. After the tests, the M-36 nickel-coated units and the Permalloy controls exhibited continuity, indicating that the electrical contact between the stator parts was not noticeably affected. However, no continuity was



found on the uncoated M-36 units on which an oxide crust clearly could be observed. When the crust was scratched away at one point on the end plate and one point on the housing, continuity was achieved, thus showing that even the M-36 coating was not affected electrically at the surface contact between the two stator parts.



Figure 5. T&H test units after 14 days.

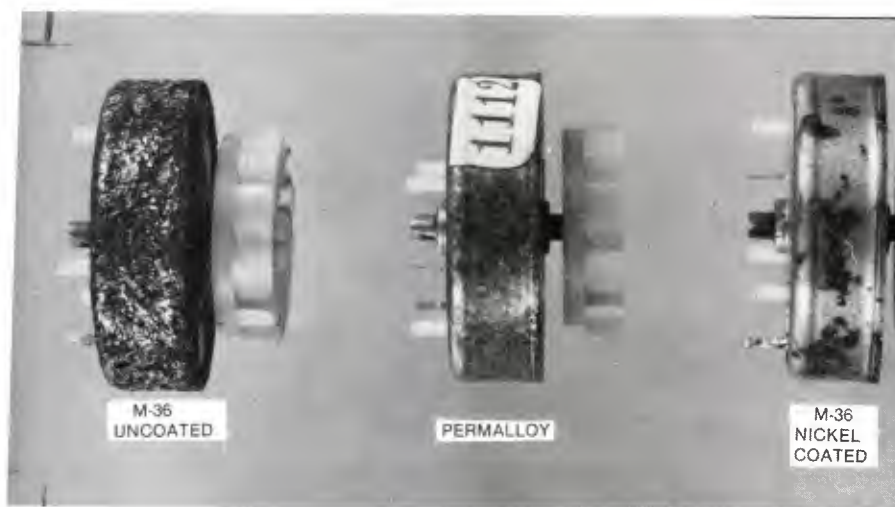


Figure 6. T&H test units after 28 days.

After completion of the T&H cycling conditioning period, the alternators were tested in the laboratory to ascertain changes in the electrical performance. It was found that the data point at 0.206 psig pressure could not be duplicated for any of the three types of alternators because the rotational speed was considerably lower after the T&H test. Disassembly of the alternators revealed rust on the shaft-bearing surface and, in some cases, rust was present into the bearings, creating excessive friction and erratic operation.

By increasing the supply pressure, the operator could obtain with difficulty a frequency close to that obtained at 0.206 psig before the T&H test. The voltages were compared at nearly the same frequency before and after the test. The results are given in table 10.

Of 11 nickel-plated M-36 alternators tested, only one, No. 36-42, had its output voltage lowered by about 1 V after the T&H test. The other 10 alternators had similar outputs before and after the test. These results showed that the nickel-plated alternators had no significant reduction in electrical voltage after T&H, thus indicating that the electrical properties of the units had not changed.

Three of the uncoated M-36 alternators that underwent the T&H test had about the same voltage and frequency levels as before. One Permalloy control unit was tested and produced the same voltage after the T&H conditioning as before.

A visual examination under a microscope was conducted on one alternator of each type after the T&H conditioning period. These alternators had not been run following the conditioning period. In summary, after the T&H test, it appears that rust appeared on all shafts at the bearing surface. The bearings themselves appeared in good condition but dry. Rust appeared in the groove

TABLE 10. COMPARISON OF ALTERNATOR OUTPUT BEFORE AND AFTER TEMPERATURE-HUMIDITY RECYCLING TEST

Alternator number	Before T&H test 0.206 psig		After T&H test	
	Freq (Hz)	Volts (rms)	Freq (Hz)	Volts (rms)
Nickel-coated units				
36-21	1402	20.4	1400	20.3
36-37	1243	20.9	1243	21.0
36-38	1309	21.0	1300	21.5
36-39	1304	20.7	1304	20.4
36-40	1310	20.7	1300	20.3
36-42	1301	20.9	1300	19.9
36-43	1296	21.3	1330	21.2
36-44	1300	21.2	1320	21.2
36-46	1301	21.0	1300	21.2
36-47	1414	20.6	1380	20.8
36-48	1379	20.3	1300	20.0
Uncoated units				
36-56	1332	21.2	1430	21.4
36-57	1319	21.8	1320	22.0
36-62	1341	21.2	1440	21.5

between the bearing and the stator cup, and, in some cases, rust got into the bearing. Thus, the reduction in frequency at 0.206 psig apparently was due to the increased friction of the rusty shafts. No rust appeared on the inside surfaces of the stators of any of the three types. This suggests that when the alternators are installed in fuzes, the additional protection will prevent significant rust from occurring. A more detailed discussion is included in appendix B.

The temperature and humidity cycling conditioning induced (a) a buildup of oxidation on uncoated M-36 stators, (b) some scattered rust on the nickel-coated M-36 stators, and (c) very little rust on the Permalloy stators. However, the electrical and magnetic properties of the uncoated or the nickel-coated M-36 stators were not affected. The Permalloy controls were likewise not affected. As a result of this test, the coating thickness on subsequent alternators was reduced to the minimum needed, so that the nickel buildup in the bearing boss or at the end plate housing contact surface was reduced.

## 6. ASSEMBLY OF ELECTRICAL STEEL STATOR ALTERNATORS FOR FIELD TEST

### 6.1 Results of Assembly at Alternator Contractor

The PIP originally called for assembly of alternators made from M-36 stators at the alternator contractor according to production assembly procedures. This was done on about 50 sets of parts, but the output of the resultant alternators as measured at the contractor's plant was reduced in both voltage and frequency.

### 6.2 Examination of Parts at HDL

An examination of the alternators and other nonassembled parts from the same batch was begun at HDL. This examination showed that the parts themselves differed in some dimensions and shapes from the Permalloy parts presently in production. It was therefore decided to assemble a group of alternators for the field test at HDL. During this assembly the discrepancies in parts could be noted and remedial procedures adopted.

This section discusses the results of this effort and the performance of the resulting alternators with electrical steel stators that were supplied for the field test. The effect on alternator performance of the dimensions that were found to be out of tolerance is shown in figure 7. This figure is a cross section of the stator assembly showing critical interfacing surfaces, alignments, and magnetic flux path. The shaft, coil assembly, and turbine have been omitted for clarity.

The interface (A) of the end plate and housing serves two purposes. It aligns the centers of the bearing holes, so that the dimension (B) should be ideally zero. If the housing shelf is not perfectly concentric with the bearing, the end plate is not perfectly concentric with its bearing. The distance (B) between the actual centers can be great enough to cause the shaft

to bind and experience excessive friction. This tends to lower the alternator output at a given air pressure. In the assembly procedure, this problem was corrected in some units by a rework in which the end plate was rotated relative to the housing so that the tolerances in the two parts would cancel. The interface (A) also is a joint through which the magnetic flux (D) from the magnet passes from the end plate to the housing, as shown. Insufficient contact surface will reduce the flux and consequently the voltage generated at a given rotational speed.

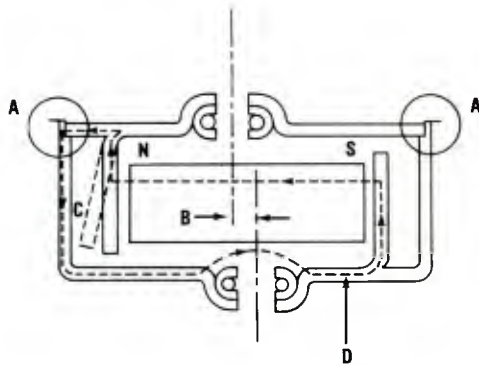


Figure 7. Cross section of stator assembly showing critical interfacing surfaces, alignments, and magnetic flux path.

The pole (C) on the end plate, if bent slightly, will increase the average distance from the magnet and increase the resistance to magnetic flux. This results in less flux in the path (D) available to cut the coil; and also reduces the voltage at a given rotational speed of the magnet. This was corrected at HDL by use of a fixture to straighten the poles.

Figure 8 shows the detail of the end plate and housing interface for Permalloy stators compared with the M-36 electrical steel. The difference is caused by the way the two materials shear at the edges, since M-36 is harder than Permalloy. The interface surface on the cylindrical part of the housing is smaller for the M-36 than for the Permalloy. This can be remedied by making dies that give sharper edges to the M-36.

A 0.002- to 0.006-in. interference fit between the end plate and housing is called for in the drawings. The diameter of the end plate is required to be 1.130 in. minimum to 1.132 in. maximum. The diameter of the shelf of the housing on which the end plate rests is 1.126 in. minimum to 1.128 in. maximum. This results in an allowed interference fit that can vary from 0.002 in. for some units to 0.006 in. for other units. On some inspected parts, the end plates were slightly larger in diameter and the housing shelves were slightly smaller in diameter, resulting in an increased interference above 0.006 in. between the parts. This increased the misalignment between the bearing holes for the out-of-round parts as described previously. The other effect was to increase the outward bowing of the end plate, which effectively gives the shaft greater axial play. The allowed tolerance range is from 0.001 to 0.013 in., and most units assembled at HDL for the field test varied between 0.010 to 0.013 in.



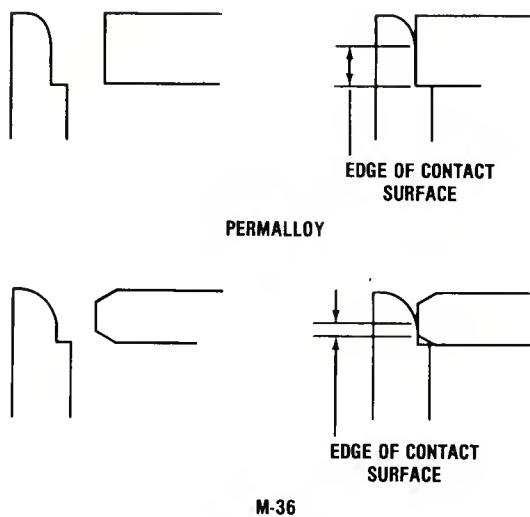


Figure 8. Comparison of end plate and housing interface for Permalloy and M-36.

### 6.3 Corrective Measures

Two gauges were made to aid in selective assembly of the alternator: one gauge for the end plate, and the other for the housing.

The gauge for the end plate consisted of a pin concentric with a cup. The pin was designed to fit the bearing that was mounted in the end plate. The cup diameter equaled the maximum allowed diameter of the end plate plus the maximum allowed tolerance of concentricity between the bearing cup and the end plate diameter. Each end plate bearing assembly was installed in the gauge and rotated 360°. Binding or tightness in rotating the 360° indicated that the part was out of tolerance.

A disk gauge was made for the housing. The gauge also had a pin to fit the bearing. The maximum diameter of the disk was the minimum allowed diameter of the housing shelf diminished by the 0.002-in. maximum allowed "out of concentricity" between the shelf and the end plate.

The housing was installed on the gauge and rotated 360°. Any binding indicated that the part was out of tolerance.

In every unit in which the end plate and housing bearing subassemblies fit tightly in the respective gauges, the alternator shaft was too tight, and the output was sharply reduced. Alternators for which the gauges were loose could be adjusted to provide the required performance. In some cases it was necessary to reorient the end plate and housing by 120° as described above.

For several units that were too tight with the noted binding of the shaft in the assembled configuration, another corrective measure was used. The housing shelf was machined to increase the undersized diameter within the

drawing tolerance and make the shelf longer as in the Permalloy housing (fig. 8). This resulted in some improved output when the housings were reannealed.

In some cases the end plate edges were filed to make a flatter edge as with the Permalloy parts (fig. 8). This produced very little improvement in output.

#### 6.4 Effect of Tight Shaft on Parameter Adjustment

The adjustment of an alternator affects the ability to obtain a certain frequency and voltage at a set pressure.

The tightness in the shaft and bearings affects the adjustment procedure as follows: The rotor must overcome the bearings' mechanical friction and the magnetic attraction between the rotor and stator poles, which increases with the flux density in the airgap. The purpose of the adjustment is to reduce the flux density in the airgap by partially demagnetizing the rotor. This allows the rotor to spin faster for the same air input. If the friction is too great, too much magnetism must be removed in order to achieve the minimum of 25,000 rpm at 0.206 psig; and the generated voltage drops too low to power the fuze electronics. The voltage increases with increasing rotational speed and increasing flux density in the airgap. Although the flux in the airgap is reduced in adjustment operation, the voltage still increases for a while because of the increasing rotational speed. Further reduction in flux density lowers the voltage.

The specifications indicate that at a pressure of  $0.206 \pm 0.003$  psig, a frequency of 1300 to 1450 and a voltage of 21.0 V or higher is indicated. More information on parameter adjustment is included in appendix A.

The core losses within the stator material increase with increasing flux density and rotational speed. The losses are greater for the electrical steel than for the Permalloy; hence, the increase in rotational speed may increase the losses more in electrical steel than in Permalloy.

#### 6.5 Condition of Alternators Assembled at HDL for Field Test

At the supply pressure of 0.206 psig, the frequency values of the 51 alternators fabricated for the field test averaged  $1279 \pm 25$  Hz and the corresponding voltage was  $20.1 \pm 0.3$  V. Although the frequencies and voltage values were averaged together, they really represented several subgroups, designated by the nature of the rework during the assembly process.

Eight alternators that had the housing shelf machined and were reannealed had higher output voltages of  $20.7 \pm 0.3$  V. Five units that had the shelf machined but were not reannealed had voltages of  $20.04 \pm 0.15$  V. It was therefore necessary to reanneal these housings after machining in order to obtain the proper output.

The remaining 38 alternators either (1) were assembled as is or (2) were reworked by disassembling before the weld operation, and reassembling with a reoriented housing and end plate and a demagnetized and recharged magnet. The average of this group is  $20.08 \pm 0.21$  V.

The output of these units is, on the average, 1 V below the minimum required 20.80 V. However, the frequencies of all units fall in the range of 1250 to 1400 Hz, as required.

## 7. FIELD TEST RESULTS ON NICKEL-COATED STATOR ALTERNATORS

A field test was conducted using 48 of the alternators described in the previous section. The purpose of the test was to verify that the alternators having the coated electrical steel stators would operate the fuze when fired over the extremes of the gun environment. The alternators had been assembled into fuzes by the fuze contractor. The test was run in conjunction with a lot-acceptance test at Jefferson Proving Ground in August 1981.

The results are summarized in table 11. The units were temperature conditioned at the extremes specified in the applicable military specification, and were fired at the lowest and highest charge zones. All units were set to detonate in the proximity mode. All but two of the fuzes functioned properly, with a distribution of burst heights similar to that obtained for the lot acceptance rounds having Permalloy stators.

The two improper fuze functions occurred at charge zone 0, 45° quadrant elevation (QE), and both were duds. One dud was heard during the first 2.1 s of flight. An examination of the arming data taken for these fuzes at the fuze contractor's plant and the performance data taken at HDL indicated no anomalous behavior that might have caused the duds. One was conditioned at ambient temperature; the other at -25 F.

The cause(s) of the duds was never determined. Even if both had been caused by the alternator, it is unlikely that the difference would be attributed to the stator material. There were two heard duds\* and one early function out of 128 rounds fired in the lot-acceptance fuzes which served as Permalloy controls. One dud occurred at charge 0, conditioned at -25 F, when fired at 45° QE, and the other occurred at charge 4, conditioned at +145 F, when fired at 45° QE. The early function occurred for a round that had been conditioned at +145 F and fired at charge 4 with a QE of 85°.

These results demonstrate that the nickel-coated M-36 stator material withstands the gun environment and provides adequate voltage for the fuzes, even though the alternator outputs as recorded in the previous section average 2 V less than the alternators with Permalloy stators.

---

\*In a "heard" dud, the alternator is known to have powered the fuze electronics.

TABLE 11. SUMMARY OF FIELD TEST DATA ON LOW-COST STATOR MATERIAL

Temp (F)	Charge	QE(°)	Total	No. of proper functions	Burst height	No. of impacts	No. of duds
Ambient	0	45	9	8	7.8 ± 2.4	0	1
-25	0	45	9	8	6.6 ± 2.4	0	1
Hot	4	45	10	10	8.1 ± 4.6	0	0
Ambient	4	45	10	10	9.1 ± 3.0	0	0
-25	4	45	10	10	7.1 ± 6.3	0	0

## 8. CONCLUSIONS AND RECOMMENDATIONS

M-36 silicon electrical steel is a suitable substitute for the Permalloy material used in the alternator stator. It can be stamped and plated with a thin coating of nickel. Severe T&H testing showed that the corrosion resistance is quite similar to that of Permalloy. The assembled alternators using such stators can be adjusted within the specified frequency and voltage range. A field test showed that these alternators survived the gun environment and satisfactorily powered the fuze.

Although variations in the grade of electrical steel from M-36 to M-45 do not reduce the electrical output, they do affect the stamping properties. Even for the M-36 material, the production dies must be developed to allow for (1) differences in the stamping and drawing properties from those of Permalloy and (2) the buildup of nickel coating in the bearing boss and at the end plate and housing contact surface. Appropriate dimensional changes will then produce proper parts without the need for corrective assembly procedures.

Before implementing this material change, an estimate in terms of time and cost should be made for producing a lot of at least 5000 alternators using nickel-coated M-36 electrical steel stators. The cost estimate should include the cost of (1) designing and fabricating new dies, (2) purchasing and installing a batch process for coating the stators, and (3) conducting a full range of alternator first-article and lot-acceptance testing. If this cost is less than the cost savings to be realized by the change when computed over the remaining fuze buys, then the material change should be validated by the testing procedure cited above and incorporated into the production line.

Since the electrical steel is difficult to draw into a cup after stamping, we conclude that the electrical steel is not easily interchangeable with Permalloy in the present production dies. However, it may be used as a substitute material in a mobilization situation if the above procedures for developing new dies are followed.



APPENDIX A.--ALTERNATOR PARAMETER ADJUSTMENT

## CONTENTS

	<u>Page</u>
A-1. REASON FOR STUDY .....	35
A-2. SEMIEMPIRICAL MODEL OF ALTERNATOR SOURCE PARAMETERS .....	35
A-3. ALTERNATOR PARAMETER ADJUSTMENT IN LABORATORY .....	39
A-4. USE OF THEVENIN EQUIVALENT CIRCUIT TO ESTIMATE ADJUSTMENT LEVEL .....	41

## FIGURES

A-1. Assumed Thevenin equivalent circuit of alternator in series with a resistive load .....	36
A-2. Operation at 0.206-psig pressure with 600- $\Omega$ load yields 1330 Hz .....	36
A-3. Operation under open-circuit load with pressure adjusted to produce 1330 Hz gives open-circuit voltage .....	36
A-4. Determining inductance of alternator under typical operating conditions .....	37
A-5. Thevenin equivalent circuit of typical alternator showing dependence of circuit parameters on frequency.....	38
A-6. Comparison of measured load voltage versus frequency curve with values calculated from Thevenin equivalent circuit parameters .....	39
A-7. Family of operating curves obtained at various levels of adjustment voltage for Permalloy stator units .....	42
A-8. Family of operating curves obtained at various levels of calibration voltage for M-36 stator units .....	43

## TABLES

A-1. Frequency for a Range of Resistive Loads Using Thevenin Equivalent Circuit Parameters from Figure 37 .....	38
A-2. Pressure for Permalloy Alternator at Successively Higher Adjustment Levels ( $R_L = 600 \Omega$ ) .....	40
A-3. Pressure for M-36 Alternator at Successively Higher Adjustment Levels ( $R_L = 600 \Omega$ ) .....	41
A-4. Estimation of Permalloy Alternator Flux at Three Levels of Adjustment Signal Based on Relationships from Thevenin Equivalent Circuit .....	44

## A-1. REASON FOR STUDY

As a corollary of the product improvement program described in the body of the report, a study was initiated to aid in isolating the effects of the electrical and magnetic properties of the alternator, such as voltage and frequency, from mechanical properties, such as aerodynamic torque and bearing friction. The focus was on clarifying the relationship between electrical output and flux level within the alternator.

This study had two results that were important and germane to alternator production and quality control. First, an approximate semiempirical method was developed to identify alternator source characteristics and provide a means of measuring them for each alternator. This could be done in production during the parameter adjustment operation. Second, the method established a relationship between source characteristics and flux level that could be employed at any intermediate level of the adjustment process to obtain better uniformity among alternators, and furnish data that could aid in troubleshooting when needed.

## A-2. SEMIEMPIRICAL MODEL OF ALTERNATOR SOURCE PARAMETERS

The Thevenin equivalent electrical circuit parameters allow the voltage and current at any point in a known electrical circuit such as a fuze load to be determined.<sup>1,2</sup>

In the following discussion, the Thevenin equivalent of the alternator is assumed to be a constant voltage source in series with an internal resistance and an inductance, as shown in figure A-1. The alternator output under other conditions is then calculated from these parameters and compared with measurements. The agreement between calculated and observed performance is an indication of the validity of the assumed equivalent circuit.

Consider two tests that are done on a typical alternator (serial No. 6422). First, the pressure is set at 0.206 psig,\* and a typical load voltage of 22.3 V is obtained at a frequency of 1330 Hz. The internal resistance of 58.6  $\Omega$  was obtained by the dc measurement with an ohmmeter. The values are shown in figure A-2, where the induction impedance,  $X_L$ , equals  $j2\pi fL$ , which for  $f = 1330$  is  $j8356L$ .

Second, the pressure is adjusted with an open-circuit load until 1330 Hz is again obtained, and the open-circuit voltage is measured and found to be 43.9 V. The open-circuit voltage in this case must be the same as in the first case, since the frequency is the same (fig. A-3).

<sup>1</sup>H. H. Skilling, *Electrical Engineering Circuits*, Ed. II, John Wiley & Sons, Inc., New York (1965), Ch. 11, Network Theorems.

<sup>2</sup>J. R. Ryder, *Electronic Fundamentals and Applications*, Ed. II, Prentice Hall, Inc., New Jersey (1959), Ch. 7, Four-Terminal Active Networks.

\*psig--differential pressure above ambient atmospheric pressure of 14.7 psi.

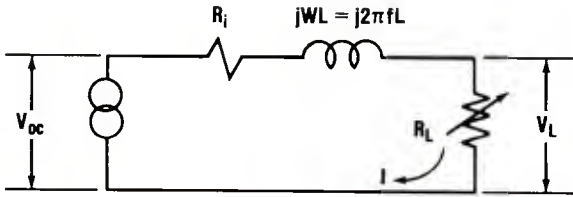


Figure A-1. Assumed Thevenin equivalent circuit of alternator in series with a resistive load.

Figure A-2. Operation at 0.206-psig pressure with 600-Ω load yields 1330 Hz.

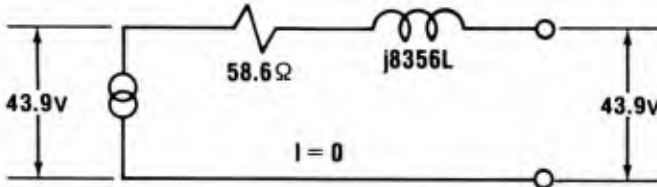
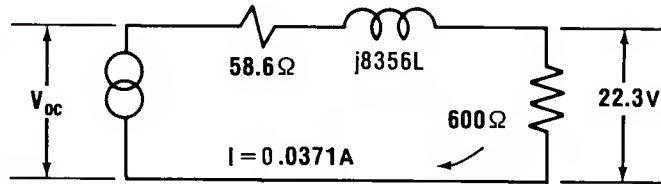


Figure A-3. Operation under open-circuit load with pressure adjusted to produce 1330 Hz gives open-circuit voltage.

The equivalent circuit of figure A-2 then becomes as shown in figure A-4(a), where the only unknown is the inductance. Since the current is known ( $22.3 \text{ V} \div 600 \Omega$ ), and the total resistance (load plus internal resistance) is known, the real part of the power can be calculated from

$$P_R = I^2 R = (0.0371 \text{ A})^2 (58.6 + 600) \Omega = 0.906 \text{ W} \quad (\text{A-1})$$

The input volt-amperes are calculated from the open-circuit voltage and the current by

$$P_I = V_{OC} I = 43.9 \text{ V} (0.0371 \text{ A}) = 1.63 \text{ W} \quad (\text{A-2})$$

The relationship between these values and the unknown reactive power is shown by the power triangle in figure A-4(b).

The phase angle can be calculated and the reactive power  $Q$  can be determined from trigonometry. For these parameters,

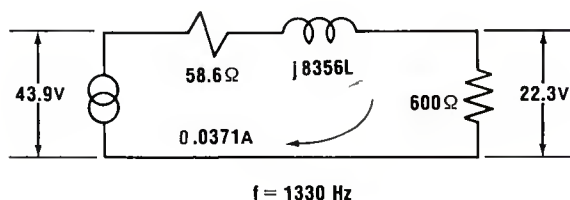
$$Q = 1.356 \text{ V-A, reactive} = I^2 X_L = I^2 2\pi f L \quad (\text{A-3})$$

Equation (A-3) can be solved for  $L$ , since  $I = 0.0371 \text{ A}$ , and  $f = 1330 \text{ Hz}$

$$L = Q / I^2 2\pi f = 1.356 / (0.0371)^2 2\pi 1330 = 0.118 \text{ H} \quad (\text{A-4})$$

The inductance is assumed to be constant, independent of frequency, so that the inductive reactance increases linearly with frequency.

The open-circuit voltage from the previous section is proportional to the frequency, so that the open-circuit voltage at any frequency,  $f$ , other than 1330 Hz may be obtained by multiplying  $V_{OC}$  (at 1330 Hz) by  $f/1330$ .



(A) EQUIVALENT CIRCUIT OF ALTERNATOR SHOWING PARAMETERS OBTAINED FROM FIRST TWO OPERATING TESTS, WITH INDUCTANCE  $L$  TO BE DETERMINED

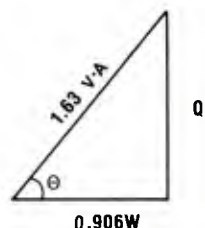


Figure A-4. Determining inductance of alternator under typical operating conditions.

(B) POWER TRIANGLE TO SOLVE FOR REACTIVE POWER  $Q$

Thus, the load voltage may be obtained at any other frequency and any known load by use of the Thevenin equivalent circuit of figure A-5. The passive load shown is resistive, but it may be any known combination of resistances and reactances. Known active elements in the load may be handled by reciprocal techniques, since the alternator source characteristics are now known.

Table A-1 is a tabulation of the expected voltages across a range of resistive loads for various frequencies, as calculated from the circuit of figure A-5. The values are plotted together with the measured curve in figure A-6. The measured curves are obtained from an xy recorder trace in which the y-axis is proportional to voltage and the x-axis is proportional to frequency. Each curve is generated by adjusting the pressure in an apparatus similar to figure 5 in the body of the report from 0 to 6 psig. The close agreement for frequencies up to 5000 Hz expected in flight shows that the assumed Thevenin equivalent circuit is a good model for the electrical source characteristics of the alternator.

This discussion was relegated to an appendix because of the nature of several assumptions and the limited scope of the effort. The primary assumptions made are that the load is resistive, that the input waveform is sinusoidal, and that the losses are independent of current and frequency.

# APPENDIX A

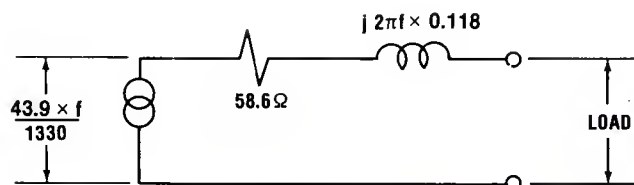


Figure A-5. Thevenin equivalent circuit of typical alternator showing dependence of circuit parameters on frequency.

TABLE A-1. FREQUENCY FOR A RANGE OF RESISTIVE LOADS USING THEVENIN EQUIVALENT CIRCUIT PARAMETERS\* FROM FIGURE 37

Freq (Hz)	$V_{OC}$ (rms)	$X$ ( $\Omega$ )	$R_L$ ( $\Omega$ )	$V_L$ (rms)
1000	33.0	741	250	10.27
			600	19.97
			1000	25.53
			2500	30.97
1500	49.51	1112	250	10.72
			600	22.98
			1000	32.24
			2500	44.36
2000	66.01	1482	250	10.90
			600	24.42
			1000	36.24
			2500	55.81
3000	99.02	2224	250	11.02
			600	25.61
			1000	40.20
			2500	73.02
4000	132.03	2965	250	11.07
			600	26.08
			1000	41.93
			2500	84.28
5000	165.03	3707	250	11.09
			600	26.29
			1000	42.80
			2500	91.59

\* $V_{OC}$  = open-circuit voltage.

$X$  = inductive reactance =  $2 \pi f L$ ;

$f$  is frequency of electrical signal (Hz);

$L$  is inductance (H).

$R_L$  = load resistance.

$V_L$  = load voltage.

The resistive load is representative of the laboratory and production testing of the alternator. The alternator waveform is sinusoidal for the resistive loads considered. However, the alternator as a fuze power supply drives a full wave bridge rectifier, which introduces higher harmonics that distort the generator waveform into nearly a square wave. Thus, the model might not work as well with such a load.



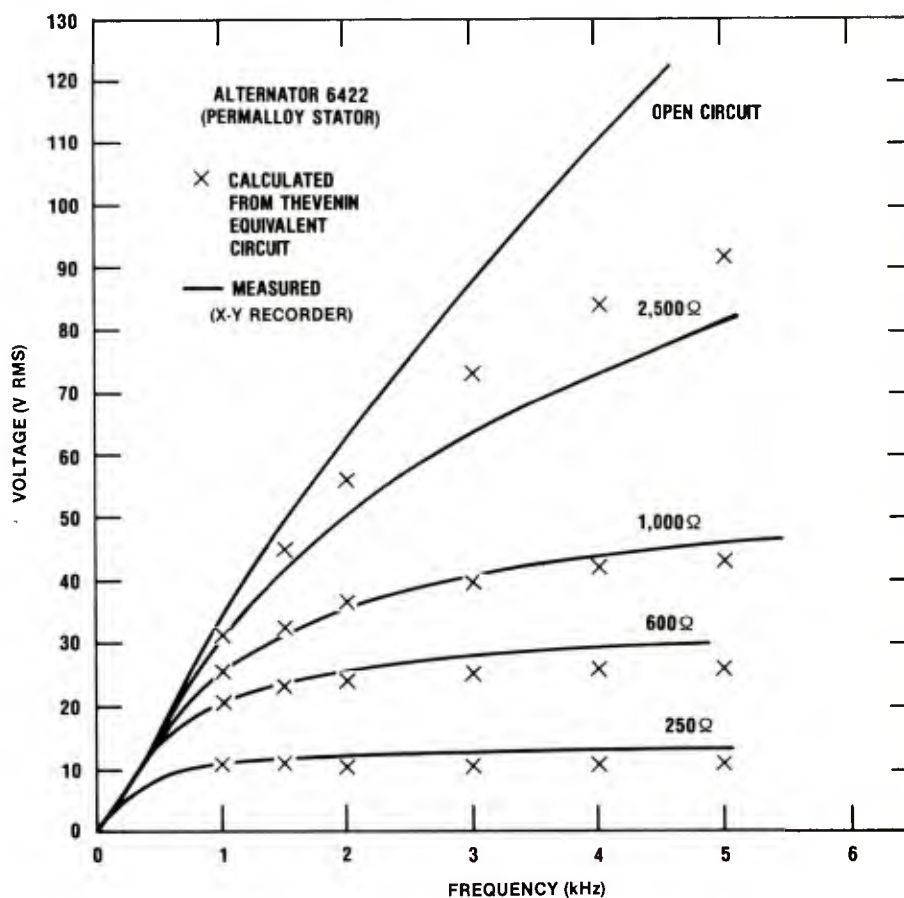


Figure A-6. Comparison of measured load voltage versus frequency curve with values calculated from Thevenin equivalent circuit parameters.

The copper losses ( $I^2R$ ) are really current dependent and may, therefore, be greater at lower resistive loads. Hence, the predicted voltages are slightly higher than the observed values at high resistance load (2500  $\Omega$ ) and are slightly lower than the observed value at the low-resistance loads (250, 600, and 1000  $\Omega$ ).

The combined core losses of the stator are not constant, but increase as a power of frequency, and therefore contribute to the difference between the measured and calculated voltage. Nevertheless, in spite of these assumptions, the model is quite good within 15 percent over the entire frequency and resistive-load range and may be used as a starting point for more extensive analysis.

### A-3. ALTERNATOR PARAMETER ADJUSTMENT IN LABORATORY

To adjust the parameters in the laboratory, the alternator, as described previously, is operated at constant pressure (0.206 psig), and the degaussing level is increased until the proper frequency range and voltage level are

# APPENDIX A

obtained. The voltage-frequency-pressure relationship at that point then determines the operation of the alternator as a fuze power supply. In this test, the voltage-frequency-pressure relationships were obtained at intermediate adjustment levels as well as at the final point.

The operating characteristics of an alternator at different adjustment levels were measured for one Permalloy stator unit and one uncoated M-36 stator unit in the preliminary phase of the program. For each alternator, voltage and frequency were recorded for several pressure values. The data are shown in table A-2 for the Permalloy unit and in table A-3 for the M-36 unit.

The voltage versus frequency curves at the various adjustment levels are plotted in figure A-7 (p 42) for the Permalloy alternator. At a given adjustment level the voltage increases with frequency. As continuous adjustment reduces the flux of the system, the voltage is lowered, and increases more gradually with frequency. Dashed lines have been drawn between points obtained at the same pressure. At a given pressure, for example 0.206 psig, the voltage first increases with increasing adjustment, reaches a maximum, and then decreases. At a given pressure, increasing the adjustment signal always increases the alternator frequency.

TABLE A-2. PRESSURE FOR PERMALLOY ALTERNATOR AT SUCCESSIVELY HIGHER ADJUSTMENT LEVELS ( $R_L = 600 \Omega$ )

Adjustment level in order of increasing signal	$\Delta P^*$ (psig)	Freq (Hz)	Volts (rms)	Adjustment level in order of increasing signal	$\Delta P$ (psig)	Freq (Hz)	Volts (rms)
0	0.206	690	20.4	4	0.165	1000	18.8
	0.25	950	24.6		0.206	1370	21.7
	0.262	1000	25.7		0.25	1680	23.4
	0.30	1300	28.8		0.30	1920	24.5
	0.40	1850	32.8		0.40	2250	25.6
1	0.206	805	21	5	0.142	1000	16.8
	0.235	1000	23.8		0.206	1480	20.8
	0.30	1500	28.5		0.25	1750	22.0
	0.40	1950	31.3		0.30	2000	23.1
					0.40	2300	24.0
2	0.206	960	21.6	6	0.13	1000	15.9
	0.215	1000	22.6		0.206	1620	19.5
	0.25	1280	25.2		0.25	1850	20.4
	0.30	1650	27.8		0.30	2080	21.2
	0.40	2060	30.0		0.40	2400	22.0
3	0.195	1000	21.3	7	0.112	1000	14.0
	0.206	1100	22.4		0.206	1700	17.6
	0.25	1400	24.8		0.25	1900	18.2
	0.30	1740	26.8		0.30	2120	18.8
	0.40	2140	28.6		0.40	2400	19.5

\*Differential pressure



TABLE A-3. PRESSURE FOR M-36 ALTERNATOR AT  
SUCCESSIVELY HIGHER ADJUSTMENT LEVELS ( $R_L = 600 \Omega$ )

Adjustment level in order of increasing signal	$\Delta P^*$ (psig)	Freq (Hz)	Volts (rms)	Adjustment level in order of increasing signal	$\Delta P$ (psig)	Freq (Hz)	Volts (rms)
0	0.206	620	19.8	5	0.18	1000	20.1
	0.25	920	24.9		0.206	1300	22.2
	0.264	1000	26.2		0.25	1550	23.6
	0.30	1250	28.8		0.30	1850	24.9
	0.40	1850	33.0		0.40	2200	26.2
1	0.206	780	21.3	6	0.15	1000	17.7
	0.24	1000	24.5		0.206	1400	20.4
	0.25	1130	25.8		0.25	1700	21.9
	0.30	1500	28.7		0.30	1940	22.7
	0.40	1960	31.3		0.40	2250	23.7
2	0.206	920	22.0	7	0.143	1000	16.8
	0.22	1000	23.2		0.206	1500	19.7
	0.25	1300	25.7		0.25	1780	20.8
	0.30	1600	27.9		0.30	2000	21.6
	0.40	2050	30.0		0.40	2350	22.5
3	0.195	1000	21.3	8	0.13	1000	15.3
	0.206	1100	22.0		0.206	1600	18.3
	0.25	1450	24.8		0.25	1850	19.2
	0.30	1720	26.3		0.30	2050	19.7
	0.40	2150	28.1		0.40	2350	20.5
4	0.186	1000	20.6				
	0.206	1200	22.1				
	0.25	1530	24.3				
	0.30	1800	25.5				
	0.40	2200	27.0				

\*Differential pressure

These curves also show that as the adjustment continues, which removes more flux from the system, lower pressures are required to produce a given frequency.

These observations also apply to alternators built using the M-36 stator material (fig. A-8, p 43).

#### A-4. USE OF THEVENIN EQUIVALENT CIRCUIT TO ESTIMATE ADJUSTMENT LEVEL

Figures A-7 and A-8 show that both voltage and frequency vary with increasing adjustment signal. The open-circuit voltage of an alternator is proportional to the time rate of change of flux through the coils, or

$$V_{OC} = N \, d\phi/dt, \quad (A-5)$$

where  $N$  is the number of turns in the coil for a periodic system of given frequency  $f$ , and

$$d\phi/dt = \omega\phi_0 = 2\pi f\phi_0 \quad . \quad (A-6)$$

Inserting equation (A-6) into (A-5) gives the following relationship for open-circuit voltage amplitude and flux amplitude:

$$V_{OC} = 2\pi Nf\phi_0 \quad . \quad (A-7)$$

Thus the ratio of the open-circuit voltage to the frequency is proportional to the flux amplitude:

$$V_{OC}/f = (2\pi N)\phi_0 \quad . \quad (A-8)$$

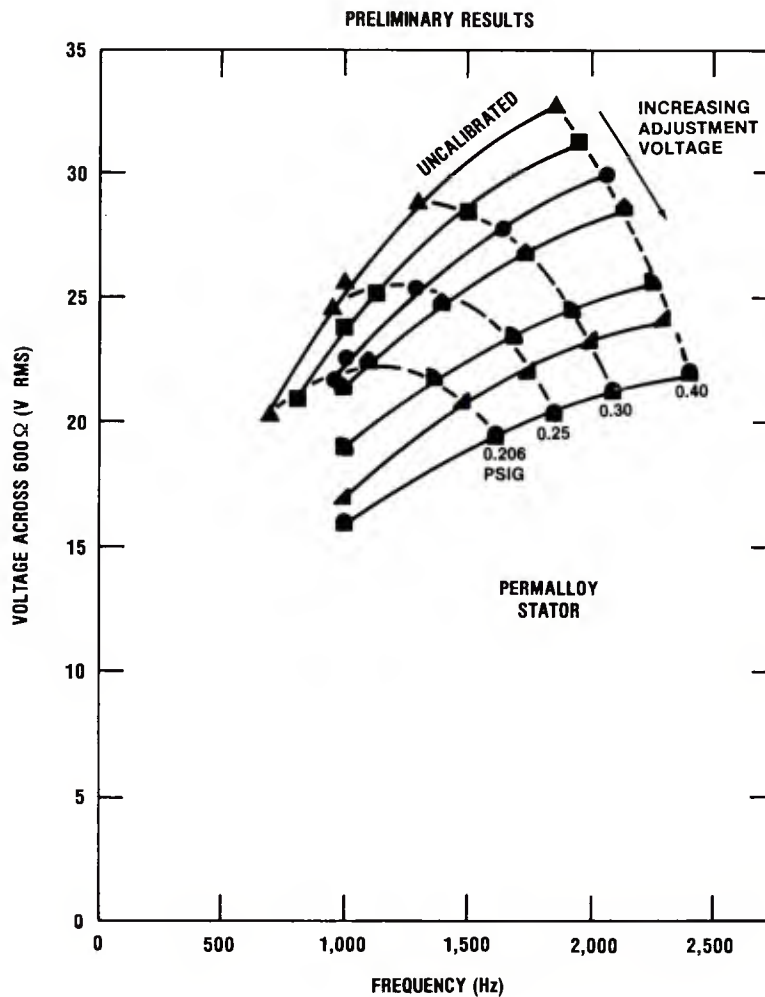


Figure A-7. Family of operating curves obtained at various levels of adjustment voltage for Permalloy stator units.

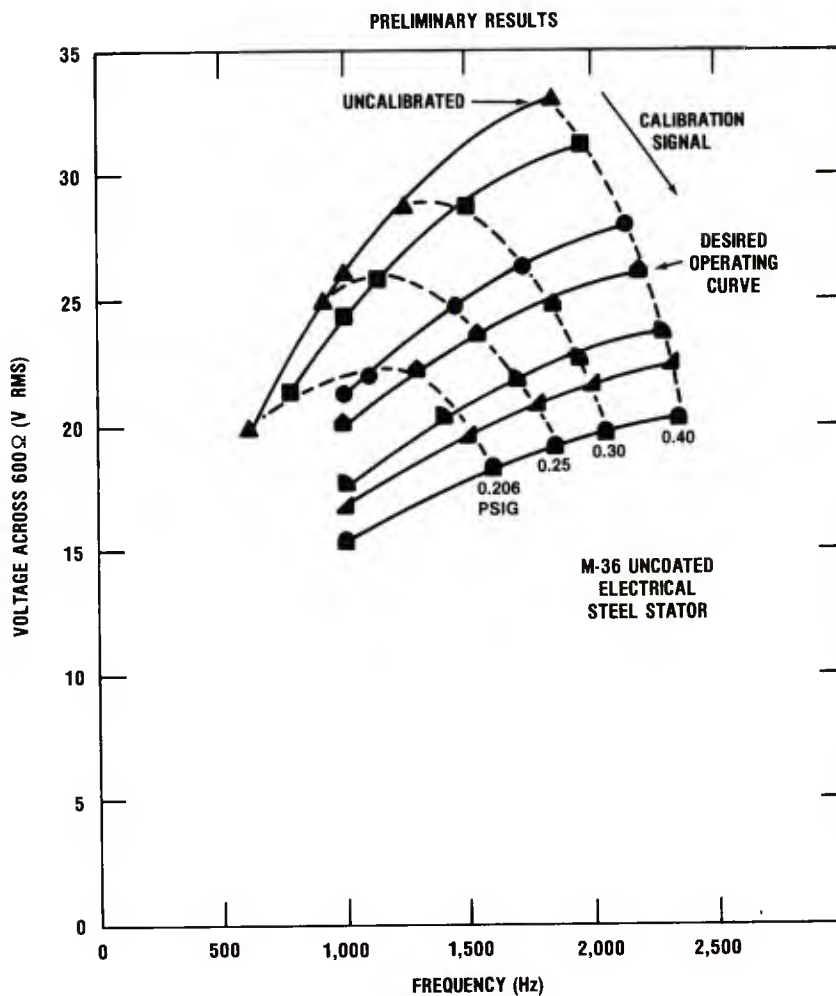


Figure A-8. Family of operating curves obtained at various levels of calibration voltage for M-36 stator units.

In this study, voltage across a 600- $\Omega$  load was measured rather than open-circuit voltage. The Thevenin equivalent circuit model furnishes a means for estimating the open-circuit voltage and the flux amplitude at each calibration level.

From the Thevenin equivalent circuit of figure A-1, the magnitude of the impedance is given in terms of the inductance, internal resistance, load resistance, and frequency by

$$|Z| = \sqrt{(R_i + R_L)^2 + \omega^2 L^2} \quad . \quad (A-9)$$

The ratio of the open-circuit voltage  $V_{oc}$  to load voltage  $V_L$  is

$$V_{oc}/V_L = |Z|/R_L = \sqrt{(R_i + R_L)^2 + \omega^2 L^2}/R_L \quad . \quad (A-10)$$

Solving for the open-circuit voltage gives

$$V_{OC} = V_L(R_i + R_L/R_L) \sqrt{1 + [\omega^2 L^2 / (R_i + R_L)^2]} \quad (A-11)$$

Thus, the open-circuit voltage can be obtained in terms of  $V_L$  from equation (A-11) at any frequency  $\omega$ , provided that the inductance  $L$ , internal resistance  $R_i$ , and load resistance  $R_L$  are known.

The flux amplitude is obtained by dividing  $V_{OC}$  by  $N\omega = 2\pi fN$ , where  $N = 600$  turns. Although  $R_i$  and  $L$  were not measured, they are assumed to be approximately equal to the values obtained in alternator No. 6422 above, nominally  $55 \Omega$  and  $0.12 \text{ H}$ , respectively.

By using these values of  $R_i$  and  $L$  in equation (A-11), the open-circuit voltage and flux amplitude were estimated for the tabulated data, and are shown in table A-4. The average flux amplitude for each calibration level is constant to within  $\pm 5$  percent, and decreases with increasing adjustment signal, as expected.

TABLE A-4. ESTIMATION OF PERMALLOY ALTERNATOR FLUX AT THREE LEVELS OF ADJUSTMENT SIGNAL BASED ON RELATIONSHIPS FROM THEVENIN EQUIVALENT CIRCUIT

Adjustment level in order of increasing signal	$\Delta P$ (psig)	$f$ (Hz)	$V_L$ (V rms)	$\omega$ (s <sup>-1</sup> )	$V_{OC}$ (V rms)	$\frac{V_{OC}}{\omega}$	$\phi_O$ ( $\times 10^{-6}$ webers)
0	0.206	690	20.4	4335	28.39	0.006549	10.915
	0.25	950	24.6	5969	39.7	0.00665	11.085
	0.262	1000	25.7	6283	42.7	0.00679	11.326
	0.30	1300	28.8	8168	56.49	0.00691	11.526
	0.40	1850	32.8	11,623	84.10	0.00723	12.06
							11.384 $\pm$ 0.444
4	0.165	1000	18.8	6283	31.24	0.00497	8.286
	0.206	1370	21.7	8607	44.16	0.00513	8.551
	0.25	1680	23.4	10,555	55.55	0.00526	8.771
	0.30	1920	24.5	12,063	64.77	0.00537	8.948
	0.40	2250	25.6	14,137	77.47	0.00548	9.133
							8.737 $\pm$ 0.331
7	0.112	1000	14.0	6283	23.26	0.0037	6.170
	0.206	1700	17.6	10,681	42.15	0.00394	6.577
	0.25	1900	18.2	11,938	47.70	0.00399	6.659
	0.30	2120	18.8	13,320	54.04	0.00405	6.761
	0.40	2400	19.5	15,079	62.44	0.00414	6.901
							6.613 $\pm$ 0.275

$\Delta P$  = differential pressure

$f$  = frequency

$V_L$  = load voltage

$\omega$  = angular frequency =  $(600) 2\pi f$

$V_{OC}$  = open-circuit voltage

$\phi_O$  = flux amplitude

$R_i$  = internal resistance of alternator =  $55 \Omega$

$R_L$  = load resistance =  $600 \Omega$

$N$  = number of turns in coil

$$R_i + R_L = 655 \Omega$$

$$(R_i + R_L)/R_L = 1.09$$

$$V_{OC} = \frac{(R_i + R_L)}{R_L} V_L \sqrt{1 + \frac{\omega^2 L^2}{(R_i + R_L)^2}}$$

$$\phi_O = \frac{V_{OC}}{N\omega}$$

APPENDIX B.--EXAMINATION OF TURBOALTERNATORS USED IN  
TEMPERATURE AND HUMIDITY TEST



This appendix describes in detail the observations of temperature and humidity testing described in section 5 in the body of the report.

Alternators were placed in a tray having 18 compartments, or cubicles, numbered from 1 to 18. In the turboalternator nomenclature, the 36 prefix designates the M-36 silicon steel stator material, and the two-digit suffix is the alternator number.

Cubicle 2      M-36, Nickel coated  
T/A 36-18

Housing. No rust marks except near weld.

End plate. Very little scaling on inside surface of end plate. Some scaling on edge near welds and between welds.

Shaft. Rust coat on rear bearing surface completely covers bearing race. On front (knurled) end of shaft, rust coat on front bearing race of shaft is not as complete a coat as on rear.

Bobbin. No visible evidence of rust on coil wire or bobbin contacts.

Front bearing. Balls appear clean and dry. Some rust on balls probably from shaft. No rust on inner race (retainer).

Rear bearing. Heavy rust deposits on balls and inside race (retainer), probably from shaft. Some rust on outside of bearing cup in housing.

Cubicle 4      M-36, Uncoated  
T/A 36-50

End plate. Outside flat surface had a crusty oxide coating; orange powder with shiny black scale. Inside flat surface had some orange rust (no black scale) and much of surface was not oxidized.

Outside edge in contact with housing does not appear to be oxidized; no orange or black scale. Looks normal.

Some orange rust on tips of pole pieces; otherwise, poles not rusted.

End plate bearing. Some metal chips or scales on balls. Traces of orange powder on balls. High buildup of orange powder on end plate near bearing cup. Apparently, orange powder on balls resulted from powder on end plate. Balls appear dry. Some traces of orange powder on edge of bearing retainer, but not inside.

Bobbin. Some orange powder on bobbin near tabs. No evidence of rust on bobbin contacts.

## APPENDIX B

Housing. Slight rust on shelf, more concentrated in a few spots, but shelf appears mostly clear of rust. Only traces of rust appear inside stator.

Orange rust in rear bearing retainer and on balls. Balls appear dry of oil.

Outside of housing has orange rust in form of a scale or crust, and black shiny oxide coating that makes surface rough. Parts of crusty coating are silvery and parts are orange.

Shaft magnet assembly. Rust on knurled end of shaft, some on bearing race, most between knurl and bearing race. Rust on rear bearing race. Some orange rust particles on plastic bushing, probably from shaft or bearing.

*NOTE: Particles that flaked off components during examination were magnetic since they were attracted to the tip of an apparently slightly magnetized jeweler's screwdriver. Particles then adhered to magnet rotor when screwdriver tip was brought in contact with rotor.*

Cubicle 11    Hi-perm 49  
T/A 1086

### Before disassembly (outside of stator):

End plate. Some small spots of orange rust scattered over surface.

Housing. On rear flat face, one large orange rust spot, one smaller, but not in critical locations. Traces of orange powder. Concentration of orange powder around ID of rear bearing boss. Some concentration of orange powder about halfway around ID of front bearing boss. Some scale noted at joint between end plate and housing. No evidence of corrosion on bobbin contacts. Traces of whitish oxide, most noticeable on outside of end plate.

### After disassembly:

End plate. Some orange oxide powder on edge in contact with housing shelf. Some traces of orange powder on inside flat surface. Concentration of scale between outside of front bearing race near where it contacts the cup in the stator. Inside of retainer appears free of rust. Balls appear bright and shiny; no scale or rust, except two particles which could have fallen onto the balls.

Bobbin. No evidence of corrosion on bobbin contacts.

Housing. Some orange rust on shelf and on back of shelf where end plate seats. Shelf is mostly clear of rust. Bearings look dry, but balls are shiny and bright; no evidence of rust on balls or inside retainer. Corrosion appears in groove between bearing and cup. Slight reddish tint to housing is probably due to orange dust.

Shaft magnet assembly. Knurled end of shaft has orange rust about halfway around, between the bearing surface and knurl. Bearing surface is free of rust. Slot end has rust rings around shaft just aft of race area, with a slight deposit in race area. Rotor had some rust spots scattered on all visible surfaces.

Turbine. Rust ring near bottom of hole.

#### ACKNOWLEDGEMENTS

The author acknowledges the assistance and contributions of Carl J. Campagnuolo and Frank Blodgett of Harry Diamond Laboratories, for their contributions on production assembly methods, and liaison with contractor and field test facilities.

The continued interest and participation of Joe Keller at Alinabal during the entire program is gratefully acknowledged.

DISTRIBUTION

ADMINISTRATOR  
DEFENSE TECHNICAL INFORMATION CENTER  
ATTN DTIC-DDA (12 COPIES)  
CAMERON STATION, BUILDING 5  
ALEXANDRIA, VA 22314

COMMANDER  
US ARRADCOM  
ATTN DRDAR-LCS, HAROLD CHANIN-DSWS  
PROJECT OFFICER  
BUILDING 94  
DOVER, NJ 07801

COMMANDER  
US ARMY RSCH & STD GP 'EUR)  
ATTN CHIEF PHYSICS & MATH BRANCH  
FPO NEW YORK 09510

COMMANDER  
US ARMY ARMAMENT MATERIEL  
READINESS COMMAND  
ATTN DRSAR-LEP-L, TECHNICAL LIBRARY  
ATTN DRSAR-ASF, FUZE & MUNITIONS  
SUPPORT DIV  
ROCK ISLAND, IL 61299

COMMANDER  
US ARMY MISSILE & MUNITIONS  
CENTER & SCHOOL  
ATTN ATSK-CTD-F  
REDSTONE ARSENAL, AL 35809

DIRECTOR  
US ARMY MATERIEL SYSTEMS ANALYSIS  
ACTIVITY  
ATTN DRXSY-MP  
ATTN DRXSY-RW, WILLIS  
ABERDEEN PROVING GROUND, MD 21005

US ARMY ELECTRONICS TECHNOLOGY  
& DEVICES LABORATORY  
ATTN DELET-DD  
FT MONMOUTH, NJ 07703

RELIABILITY ANALYSIS CENTER  
RADC (RBRAC)  
ATTN DATA COORDINATOR/GOVT PROGRAMS  
GRIFFISS AFB, NY 13441

BROOKHAVEN  
DEPT OF ENERGY  
ASSOCIATED UNIVERSITIES, INC  
ATTN TECHNICAL INFORMATION DIV  
ATTN PHISCS DEPT, 5103  
UPTON, LONG ISLAND, NY 11973

DEPARTMENT OF COMMERCE  
NATIONAL BUREAU OF STANDARDS  
ATTN LIBRARY  
WASHINGTON, DC 20234

NATIONAL OCEANIC & ATMOSPHERIC ADM  
ENVIRONMENTAL RESEARCH LABORATORIES  
ATTN LIBRARY, R-51, TECH REPORTS  
BOUDLER, CO 80302

OUSDR&E  
DIRECTOR ENERGY TECHNOLOGY OFFICE  
THE PENTAGON  
WASHINGTON, DC 20301

COMMANDER  
US ARMY ARMAMENT RESEARCH &  
DEVELOPMENT COMMAND  
ATTN DRCPM-CAWS, PM, CANNON ARTILLERY  
WEAPONS SYSTEMS/SEMI-ACTIVE  
LASER GUIDED PROJECTILES  
ATTN DRCPM-SA, PM, SELECTED AMMUNITION  
ATTN DRDAR-TDR, RESEARCH & TECHNOLOGY  
ATTN DRDAR-LC, LARGE CALIBER WEAPON  
SYSTEMS LABORATORY  
ATTN DRDAR-QA, PRODUCT ASSURANCE DIV  
DOVER, NJ 07801

COMMANDER  
USARRADOM  
BENET WEAPONS LAB LCWSL  
WATERVLIET, NY 12189

COMMANDER  
US ARMY COMMUNICATIONS COMMAND  
USA COMMO AGENCY, WS  
WHITE SANDS MISSILE RANGE, NM 88002

DEPARTMENT OF THE ARMY  
CONCEPT ANALYSIS AGENCY  
8120 WOODMONT AVE  
BETHESDA, MD 20014

PRESIDENT  
US ARMY FIELD ARTILLERY BOARD  
ATTN ATZR-BDWT, WEAPONS TEST DIV  
ATTN ATZR-BDAS, ARTILLERY SPT TEST DIV  
FT SILL, OK 73503

DIRECTOR  
US ARMY HUMAN ENGINEERING LABORATORY  
ATTN DRXHE-PC, TECH LIBRARY  
ABERDEEN PROVING GROUND, MD 21005

COMMANDER  
US ARMY MATERIEL DEVELOPMENT  
& READINESS COMMAND  
ATTN DRUDE, DIR FOR DEVELOPMENT & ENG  
5001 EISENHOWER AVE  
ALEXANDRIA, VA 22333



DISTRIBUTION (Cont'd)

COMMANDER  
US ARMY MATERIALS & MECHANICS  
RESEARCH CENTER  
ATTN DRXMR-PL, TECHNICAL LIBRARY  
WATERTOWN, MA 02172

COMMANDER  
US ARMY MISSILE COMMAND  
ATTN DRCPM-CF, CHAPARRAL/FAAR  
ATTN DRCPM-HD, HELLFIRE/GLD  
ATTN DRCPM-PE, PERSHING  
ATTN DRCPM-DT, TOW DRAGON  
ATTN DRCPM-RS, GENERAL SUPPORT  
ROCKET SYS  
REDSTONE ARSENAL, AL 35809

DIRECTOR  
US ARMY MISSILE LABORATORY  
USAMICOM  
ATTN DRSMI-RPR, REDSTONE SCIENTIFIC  
INFO CENTER  
ATTN DRSMI-RPT, TECHNICAL  
INFORMATION  
ATTN DRSMI-RE, ADVANCED SENSORS DIR  
REDSTONE ARSENAL, AL 35809

COMMANDER & DIRECTOR  
OFC OF MISSILE ELCT WARFARE  
ATTN DELEW-M-PM, PROG MGT SPT OFFICE  
ATTN DELEW-M-ST, SURFACE TARGET DIV  
ATTN DELEW-M-TA, TECH & ADV  
CONCEPTS DIV  
WHITE SANDS MISSILE RANGE, NM 88002

COMMANDER  
US ARMY NATICK RES & DEV COMMAND  
NATICK DEVELOPMENT CENTER  
ATTN DRDNA-T, TECHNICAL LIBRARY  
ATTN DRDNA-U, DIR AERO-MECHANICAL  
ENGINEERING LABORATORY  
NATICK, MA 01760

OFFICE OF THE DEPUTY CHIEF OF STAFF  
FOR RESEARCH, DEVELOPMENT &  
ACQUISITION  
ATTN DAMA-WSW, GROUND COMBAT  
SYSTEMS DIV  
WASHINGTON, DC 20310

COMMANDANT  
US ARMY FIELD ARTILLERY SCHOOL  
ATTN LIBRARY  
FT SILL, OK 73503

COMMANDANT  
US ARMY ENGINEER SCHOOL  
ATTN LIBRARY  
FT BELVOIR, VA 22060

COMMANDANT  
US ARMY INFANTRY SCHOOL  
ATTN LIBRARY  
FT BENNING, GA 31905

COMMANDANT  
US ARMY WAR COLLEGE  
ATTN LIBRARY  
CARLISLE BARRACKS, PA 17013

COMMANDER  
US ARMY ORDNANCE  
CENTER & SCHOOL  
ABERDEEN PROVING GROUND, MD 21005

COMMANDER  
NAVAL AIR DEVELOPMENT CENTER  
ATTN TECHNICAL LIBRARY  
WARMISTER, PA 18974

SUPERINTENDENT  
NAVAL POSTGRADUATE SCHOOL  
ATTN LIBRARY, CODE 2124  
MONTEREY, CA 93940

DIRECTOR  
NAVAL RESEARCH LABORATORY  
ATTN 2600, TECHNICAL INFO DIV  
ATTN 2750, OPTICAL SCIENCES DIV  
ATTN 5500, OPTICAL SCIE DIV  
ATTN 6000, MATL & RADIATION  
SCI & TE  
WASHINGTON, DC 20375

COMMANDER  
DAVID W. TAYLOR NAVAL SHIP R&D CENTER  
BETHESDA, MD 20084

COMMANDER  
NAVAL SURFACE WEAPONS CENTER  
ATTN DX-21 LIBRARY DIV  
DAHLGREN, VA 22448

SUPERINTENDENT  
HQ US AIR FORCE ACADEMY  
ATTN TECH LIB  
USAF ACADEMY, CO 80840

AF AERO-PROPULSION LABORATORY  
WRIGHT-PATTERSON AFB, OH 45433

COMMANDER  
ARNOLD ENGINEERING DEVELOPMENT CENTER  
ATTN DY, DIR TECHNOLOGY  
ARNOLD AIR FORCE STATION, TN 37389

DISTRIBUTION (Cont'd)

DIRECTOR

NASA  
GODDARD SPACE FLIGHT CENTER  
ATTN 250, TECH INFO DIV  
GREENBELT, MD 20771

DIRECTOR

NASA  
ATTN TECHNICAL LIBRARY  
JOHN F. KENNEDY SPACE CENTER,  
FL 32899

DIRECTOR

NASA  
LANGLEY RESEARCH CENTER  
ATTN TECHNICAL LIBRARY  
HAMPTON, VA 23665

LAWRENCE LIVERMORE NATIONAL LABORATORY  
PO BOX 808  
LIVERMORE, CA 94550

US ARMY ELECTRONICS RESEARCH  
& DEVELOPMENT COMMAND  
ATTN TECHNICAL DIRECTOR, DRDEL-CT

HARRY DIAMOND LABORATORIES  
ATTN CO/TD/TSO/DIVISION DIRECTORS  
ATTN RECORD COPY, 81200  
ATTN HDL LIBRARY, 81100 (3 COPIES)  
ATTN HDL LIBRARY, 81100 (WOODBIDGE)  
ATTN TECHNICAL REPORTS BRANCH, 81300  
ATTN LEGAL OFFICE, 97000

HARRY DIAMOND LABORATORIES (Cont'd)  
ATTN CHAIRMAN, EDITORIAL COMMITTEE  
ATTN DRDEL-IN  
ATTN MORRISON, R. E., 13500 (GIDEP)  
ATTN CHIEF, 21000  
ATTN CHIEF, 21100  
ATTN CHIEF, 21200  
ATTN CHIEF, 21300  
ATTN CHIEF, 21400  
ATTN CHIEF, 21500  
ATTN CHIEF, 22000  
ATTN CHIEF, 22100  
ATTN CHIEF, 22300  
ATTN CHIEF, 22800  
ATTN CHIEF, 22900  
ATTN CHIEF, 20240  
ATTN P. KOPETKA, 34600  
ATTN N. DOCTOR, 34600  
ATTN F. BLODGETT, 34600  
ATTN C. CAMPAGNUOLO, 34600  
ATTN P. INGERSOLL, 34300  
ATTN D. BRIGGMAN, 34300  
ATTN G. NORTH, 47500  
ATTN B. WILLIS, 47400  
ATTN R. PROESTEL, 34600  
ATTN H. DAVIS, 34600  
ATTN L. HUGHES, 34600  
ATTN M. McCALL, 34600  
ATTN S. ALLEN, 34600  
ATTN B. GOODMAN, 42440  
ATTN J. COOPERMAN, 42440  
ATTN D. SCHNEIDER, 47100  
ATTN M. FLOYD, 47400  
ATTN J. FINE, 34600 (10 COPIES)